J. Electrochem. Sci. Eng. **13(6)** (2023) 839-879; http://dx.doi.org/10.5599/jese.1713

Open Access : : ISSN 1847-9286
https://pub.iapchem.org/ojs/index.php/JESE

Review paper

Computational materials discovery and development for Li and non-Li advanced battery chemistries

Henu Sharma[1,2,✉] Aqsa Nazir[3], Arvind Kasbe[4], Prathamesh Kekarjawlekar[2], Kajari Chatterjee[2], Saeme Motevalian[3], Ana Claus[3], Viswesh Prakash[5], Sagnik Acharya[2] and Kisor K. Sahu[2,✉]

[1]*NetTantra Technologies India Pvt. Ltd, Bhubaneswar, India*
[2]*School of Mineral, Metallurgical, and Materials Engineering, Indian Institute of Technology, Bhubaneswar, India*
[3]*Department of Mechanical and Materials Engineering, Florida International University, Florida, USA*
[4]*Ecoworld Pharm, Jeollanam-do, South Korea*
[5]*Department of Metallurgical and Materials Engineering, National Institute of Technology, Karnataka, Surathkal, India*

Corresponding author: ✉hs17@iitbbs.ac.in; ✉kisorsahu@iitbbs.ac.in

Received: February 15, 2023; Accepted: October 3, 2023; Published: October 23, 2023

Abstract

Since the discovery of batteries in the 1800s, their fascinating physical and chemical properties have led to much research on their synthesis and manufacturing. Though lithium-ion batteries have been crucial for civilization, they can still not meet all the growing demands for energy storage because of the geographical distribution of lithium resources and the intrinsic limitations in the cell energy density, performance, and reliability issues. As a result, non-Li-ion batteries are becoming increasingly popular alternatives. Designing novel materials with desired properties is crucial for a quicker transition to the green energy ecosystem. Na, K, Mg, Zn, Al ion, etc. batteries are considered the most alluring and promising. This article covers all these Li, non-Li, and metal-air cell chemistries. Recently, computational screening has proven to be an effective tool to accelerate the discovery of active materials for all these cell types. First-principles methods such as density functional theory, molecular dynamics, and Monte Carlo simulations have become established techniques for the preliminary, theoretical analysis of battery systems. These computational methods generate a wealth of data that might be immensely useful in the training and validating of artificial intelligence and machine learning techniques to reduce the time and capital expenditure needed for discovering advanced materials and final product development. This review aims to summarize the application of these techniques and the recent developments in computational methods to discover and develop advanced battery chemistries.

Keywords
Machine learning; DFT; Monte Carlo simulations; artificial intelligence, molecular dynamics; metal-air batteries

Introduction

In 1987, Yoshino and his colleagues patented the first rechargeable lithium-ion battery, which Sony (a Japanese conglomerate) later commercialized. They have paved the way for the evolution of wireless portable devices such as laptops, cell phones, watches, digital cameras, and so on. For the last 20 years and counting, lithium-ion batteries (LIBs) have been the undisputed leader in the field of electrochemical energy storage. They are still one of the most highly studied fields as a great topic of interest [1]. Though, the future might not be as easy since some issues, such as high cost and limited resources, are likely to create serious impediments to meeting the future requirements of energy storage devices [2]. Rechargeable LIBs are an appealing choice for a wide range of applications due to their high energy density [3], long cycle life [4], and low self-discharge [5]. However, it has some performance issues and limitations, such as sensitivity to high temperatures, a limited number of charge-discharge cycles, and potential safety issues, *e.g.,* thermal runaways. To address these limitations [6], researchers are investigating alternative battery chemistries such as monovalent metal ion [7], multivalent metal ion [8], and metal-air [9] batteries. They are also progressively gaining popularity as one of the most dependable energy storage devices and have the potential to meet the needs of electric vehicles (EV) and other future applications [10].

Rechargeable batteries involve numerous complex electrochemical processes at diverse lengths and time scales, often spanning several orders of magnitudes, making a holistic understanding of their behavior a difficult proposition through the experimental route alone. The high cost of experimenttation, particularly those involving large-scale battery testing, is also a big factor. Computational simulations can help solve some of them to an extent. Traditional experimental tools are time-consuming and expensive. Once properly set-up, simulations can be run much faster than experiments, allowing researchers to study the behavior of systems over long periods or at high speeds. Simulations can provide a comprehensive understanding of the complex electrochemical reactions within rechargeable batteries. Furthermore, the environment can be precisely controlled, and the effects of various parameters can be studied outside of the constraints of a laboratory setting.

As depicted in Figure 1, the progression of scientific advancements can be broadly classified into 4 paradigms (i) experimental, (ii) theoretical, (iii) computational, and (iv) data-driven science. The first paradigm refers to the observation and experimentation of natural phenomena. For example, Italian physicist Alessandro Volta developed the first ever operable battery consisting of alternating silver and zinc disc-shaped plates separated by paper soaked in a solution of sodium hydroxide (now known as the “voltaic pile”) through systematic investigation of electrochemical phenomena during the 1790s. Later experiments on the voltaic pile performed by Michael Faraday led to the derivation of the quantitative laws of electrochemistry, which forms the basis of much of our understanding of modern battery technology. The second paradigm describes the development of models in theoretical science to precisely describe and explain natural phenomena and laws of sciences. The laws of thermodynamics are useful in natural sciences for describing physical quantities like temperature (*T*), energy (*E*), and entropy (*S*). The laws of thermodynamics enabled us to estimate and predict the extractable energy from a cell through a clearer understanding of the relevant free energies. During the 20th century, computers began to progress and changed the world through innovations in computational sciences. The discovery of multitudes of computational tools is the hallmark of the third

paradigm. Hohenberg and Kohn [11,12] are widely regarded inventors of the modern density functional theory (DFT, discovered in 1964). It is a quantum-mechanical atomistic simulation method used to calculate the properties of atomic systems such as atoms, molecules, crystals, and microscopic surfaces. The discovery of new materials with distinct properties and functions with the aid of computational protocols has transformed the entire research community in pure science, materials science, biomedical science, engineering science, and so on. As a sub-set, almost all aspects of battery science and technologies are also transformed, and this is the prime theme of this article. Massive amounts of material information and data have been generated by these computational and experimental tools, resulting in 'big data'. These big data are exploited by artificial intelligence (AI) and machine learning (ML) to produce meaningful results in material behaviors in science and technology, resulting in the fourth paradigm. Materials 4.0 [13] is another name for this.

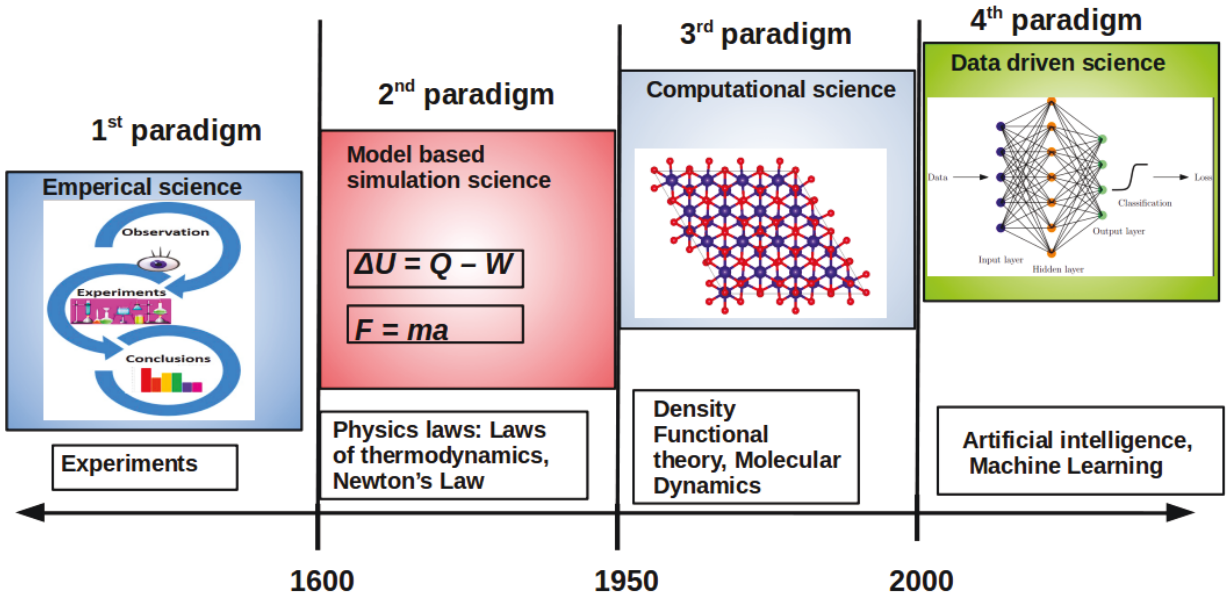

Figure 1*. The four paradigms of science through different timelines*
Copyright 2019. Adapted from Springer Nature [14]

The primary goal of this review is to provide a fundamental understanding of computational techniques (such as first-principles simulations, molecular dynamics (MD), kinetic Monte Carlo (KMC), artificial intelligence (AI), and machine learning (ML) used to design and guide the experimental synthesis of the various types of energy storage systems. Each battery chemistry is distinct, and it is critical to understand which chemistries are best suited for the required range of applications. With the help of computational simulations, it becomes easy to focus on the relative merits of different battery chemistries. Towards the end of this review, we also provide a perspective on the current issues of rechargeable batteries for energy storage devices and their potential pertinent solutions.

Traditional computational frameworks

Due to the inherent difficulty in directly observing some of the real-world phenomena, researchers and scientists developed the third paradigm in science that enables them to study these complex, time-consuming, dangerous (*e.g.,* radioactive), and inaccessible (*e.g.,* core of a star) systems using models and simulations. The third scientific paradigm, also known as "simulation-based science," emphasizes computational methods for scientific research, such as computer simulations and modeling. They can be used to test hypotheses, track individual atoms, predict

outcomes, and gain a better understanding of research work. Modern computing relies heavily on efficient algorithms and ever-increasing computational power at rapidly decreasing costs. Simulations benefit from computer processing power and algorithms to accurately model, solve, and analyze complex systems and phenomena. Algorithms, on the other hand, are sets of mathematical rules and procedures that allow a computer to perform specific tasks. Simulations can also be used to optimize designs, test the safety and performance of new products, and train researchers in a safe and controlled environment by generating different data sets.

First-principles calculations DFT

Among all rechargeable batteries, the LIB [15] is the most extensively commercialized battery type. LIBs have been recognized as vital energy storage systems for a variety of electrical devices due to their favorable electrochemical characteristics like high energy density, long life, and high power [16]. Using appropriate DFT calculations, one can begin from a given structure and gain a thorough understanding and precise prediction of material properties [17] and their reaction mechanisms. DFT is a successful approach for the practical implementation of quantum mechanics through solving the Schrodinger equation, thereby describing the behavior of atoms and molecules. The ground-state energy can be expressed as a function of electron density [11,12]. The energy of any system is made up of contributions from non-interacting nuclei, electrons, Coulombic interactions, and unaccounted effects grouped as an exchange-correlation term. The local density approximation (LDA), or the somewhat refined form of it, the generalized gradient approximation (GGA), is frequently used to approximate the exchange-correlation energy. DFT calculations can provide vital information on the charge, energy, magnetism, rate capacity, and safety of rechargeable LIBs [18,19] and non-Li batteries. They can also provide results (roughly comparable to the experiments) for lithium intercalation voltage, phase instability, charge and lithium distribution, and kinetics [20]. DFT results can also help to connect structure and its characteristics. DFT software such as VASP [21], SIESTA [22], DMOL^3 [23], Quantum Espresso [24], ABINIT [25], *etc*, are widely accepted in studying the electronic properties of rechargeable batteries. The overview of relevant works reported by different DFT tools has been summarized in Table 1.

Table 1. *Summary of computational studies of Li and non-Li advanced batteries by DFT calculations*

Materials/systems	Computational tools	Highlighted features	Ref.
Energetics studies (Li, Na, Mg)	SIESTA	• Comparison between Li, Na, Mg storage solutions in different forms (amorphous vs. crystalline) Si (*a*-Si and *c*-Si, respectively) • *a*-Si is preferable to *c*-Si for both insertion energetics and volume expansions	[26]
Sodiation studies (Si, Ge, Sn)	VASP	• In contrast to lithiation, specific atomic configurations cause the softening, volume expansion, and increase in Na diffusivity to occur more quickly with sodiation	[27]
Anchoring material study (Li-S)	DMOL^3, VASP	• g-SiC_2 inhibits the shuttle effect through a remarkable affinity for Li_2S_n species. • Gives a more precise standard for evaluating anchoring materials to prevent the shuttle effect	[28,29]
Anode material studies (Li-ion, Na-ion, Mg-ion, K-ion)	VASP, Quantum ESPRESSO	• Pre-lithiated VS_2 might be an attractive anode for LIBs. • For sodium-ion batteries boron-doped graphdiyne makes a good anode material	[30-34]

Materials/systems	Computational tools	Highlighted features	Ref.
Cathode material studies (Li-S)	VASP	• Studied the capturing process of a polysulfide (PS) by an under-coordinated carbon in the c-PAN backbone. • With increasing polymer lithiation, C-H bond strength diminishes	[35]
Adsorption studies (Na-ion)	Quantum ESPRESSO DMOL^3	• For Na-ion batteries, graphene is not a desirable anode material. • Defects can significantly enhance Na storage.	[36,37]
Negative electrode material study for Li-ion battery	ABINIT	• Total energy studies for Li-Si alloys	[38]
Electronic/Ionic transport studies ($LiFeBO_3$)	VASP	• By Hubbard-corrected DFT, the structural and kinetic characteristics of Li_xFeBO_3 were examined.	[39]

Molecular dynamics

Molecular dynamics (MD) simulation is an extremely useful tool in battery research as it provides critical information for improving battery performance and developing new battery materials and designs. In a generic sense, MD relinquishes the precise quantum calculation (to significantly reduce computational cost) and adopts a much cheaper classical approach based on Newtonian mechanics to cover much larger time and length scales. However, in some cases, it can be closely integrated with quantum calculation to retain some advantages of both worlds. In the following, we sample some examples from battery research to illustrate these points.

He *et al.* [40] performed *ab initio* molecular dynamics calculations (AIMD) simulations and topological analyses for a systematic study of super-ionic conductors (SICs) to reveal their unique key features. In addition to having a disordered Li sublattice, they found evidence of positional disordering on some sites in SICs, where the Li^+ ions move rapidly over a small area of positions in a fraction of a picosecond. These regions were labeled as “enlarged Li sites”. The Li^+ probability density calculations show ellipsoid (LGPS ($Li_{10}GeP_2S_{12}$) and LLZO ($Li_7La_3Zr_2O_{12}$)) or elongated (LATP ($Li_{1.5}Al_{0.5}Ti_{1.5}(PO_4)_3$) shapes due to the positional disordering of the ions (shown in Figure 2). These enlarged sites are commonly treated as split sites with partial occupancy and can be observed in diffraction experiments.

Using topological analyses, the researchers quantified some key features of the crystal structure framework of SICs. They observed that the percolation radii of most SICs were in the range of 0.050 to 0.075 nm and had enlarged Li sites larger than 0.22 nm, with the Li nodes connected by a short distance of about 0.25 nm. Using these parameters, the researchers were able to perform high-throughput screening of thousands of Li-containing oxides and sulfides from the Inorganic Crystal Structure Database (ICSD) [41] by following a 6-step process, ending up with 76 crystal structures that shared the same features as known fast Li-ion conductors.

Dawson *et al.* [42] used large-scale MD simulations to study the effects of grain boundaries (GBs) on Li-ion conductivity in the solid electrolyte Li_3OCl. They chose four symmetric tilt GBs observed in various other perovskite samples used as solid electrolytes. They observed that the calculated GB energies for Li_3OCl are very low compared to other perovskites due to the ease of breaking the Li-O or Li-Cl bonds and the fact that Li can adjust in various coordination environments.

These low energies hint at the higher occurrence of GBs in Li_3OCl, contributing to high GB resistance.

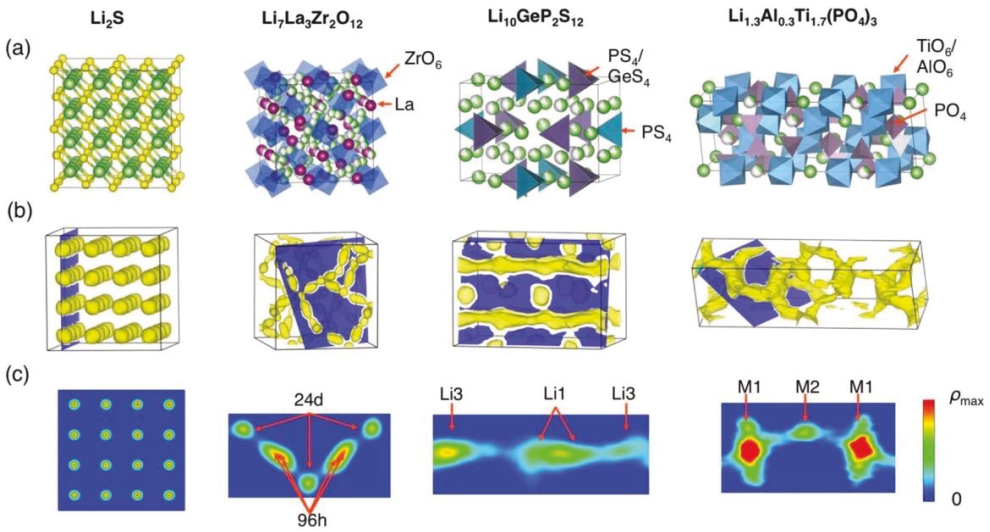

Figure 2. *(a) Crystal structures of Li_2S, LLZO, LGPS, and LATP, (b) Li^+ probability density at 900K, (c) Li^+ probability density (cross-section) from the blue plane in (b) [40]*
Copyright 2019. Reproduced with permission from John Wiley and Sons

Using their calculated conductivities, a phenomenological model was built to account for the effects of GBs on a polycrystalline material. They elucidated that ion conduction occurs through two competing processes in such a material: (i) the granular pathway, which dominates when the GBs have much larger resistance than the bulk crystalline portions, and (ii) the GB pathway, which occurs when conduction in GBs is comparable in magnitude to the bulk electrolyte (*e.g.,* in some sulfides and solid oxides), as shown in Figure 3 (a) and (b).

They plotted the total conductivity of Li_3OCl against grain size (shown in Figure 3c), which revealed two main features: (i) conductivity enhances with the increase of the grain size of the polycrystalline material (expected because the GBs contribute to significant resistance in the material), and (ii) GB resistances are shown to be very large at particle sizes <100 nm and bulk conductivity starts dominating around ~400 nm. Figures 3 (d), (e) and (f) depict MD simulations of the Li transport near the GBs and bulk Li_3OCl. From the images, we can see that initially, the Li-ions close to the GBs move only in the x and y directions. Over time, some of these ions propagate into the bulk medium. By 10 ns, the trajectories are very similar to vacancy migration seen in bulk Li_3OCl.

Monte Carlo and kinetic Monte Carlo

Advances in improving the performance of LIBs are pushing the frontiers of materials design from the nano-, to micro- to system-scales. Therefore, it is important to connect and understand how atomic events affect the electrochemical behavior of storage devices. These atomic events represent chemical reaction processes such as adsorption, desorption, and diffusion events. Kinetic Monte Carlo (KMC) is a powerful dynamic modeling technique that uses a stochastic approach to simulate the chemical reaction processes, where a reaction process is chosen based on a probability distribution representing its rate constant. By virtue of doing away from the atomic description in favor of probability distribution, KMC allows us to run simulations at longer time scales without necessarily losing all the configurational atomic details and retaining only the important aspects. Figure 4 shows the general steps involved in running a simple KMC simulation.

Zhang *et al.* [44] developed an electrochemical model to study the dendrite growth owing to the deposition of Li considering various factors such as porosity, solid electrolyte interface (SEI) thickness, and some external conditions. They have considered two processes for deposition, Li dendrite growth and Li plating.

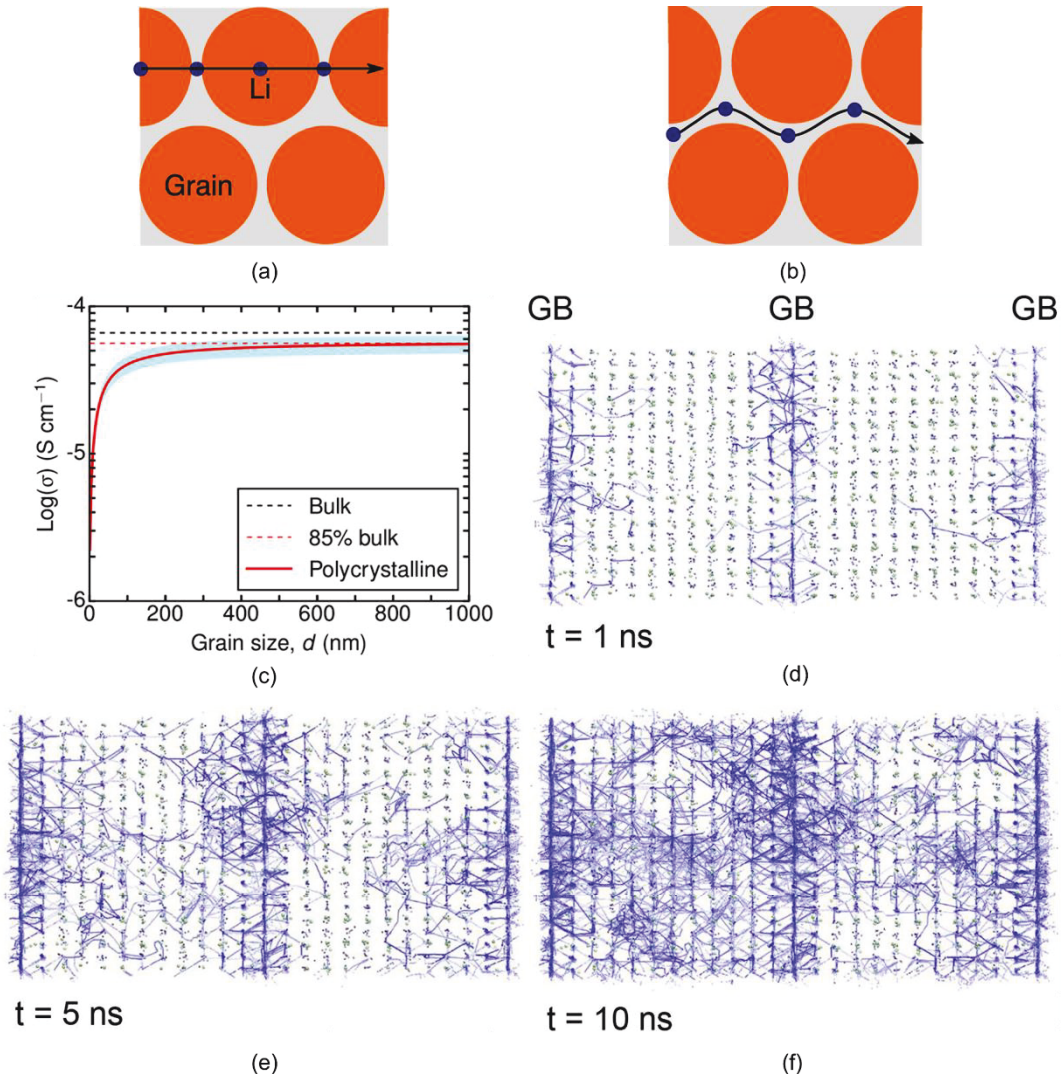

Figure 3. *(a) Granular conduction (b) GB conduction pathways for Li ions. The orange areas represent the grains, the gray areas are GBs, and the blue particles are Li ions, (c) Total conductivity of Li_3OCl as grain size changes at 300K, (d), (e) and (f) are Li-ion density maps showing the trajectories of Li-ions near the GBs and bulk Li_3OCl. Copyright 2018. Reproduced with permission from ACS Publications [42]*

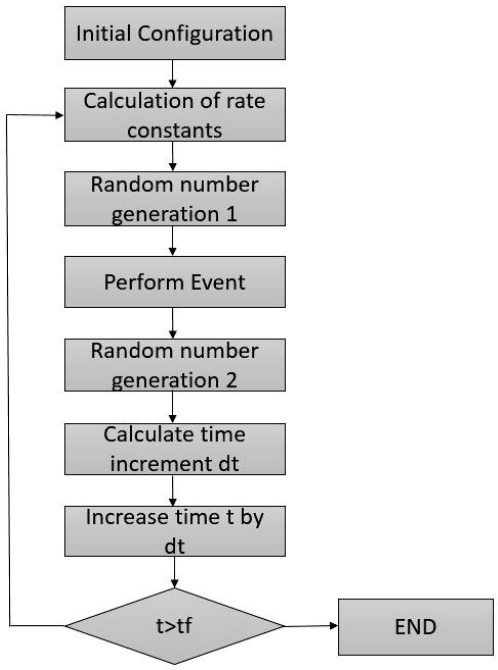

Figure 4. *Flow chart of KMC simulation [43]. Copyright 2021. Adapted from IOP Publishing Ltd*

Dendritic Li deposition consumes recyclable active Li^+ content, leading to increased resistance, power, and capacity degradation [45,46]. One of the greatest risks emerges when the separator is punctured by Li dendrites, leading to an electrical short-circuit and potentially leading to an accident [47]. By considering various surfaces of a single crystal with the help of the kMC-embedded atom technique, Ghalami *et al.* [48] explored the electrodeposition of Li onto metallic Li.

Using a metal anode directly in rechargeable batteries will significantly improve the energy density. The morphological evolution of the electrode surface is one of the primary challenges in commercializing such batteries. It is well known that electrode surfaces in Li anode-based LiBs are prone to dendrite formation, which lowers electrochemical activity and results in failure by producing electric short circuits. Numerous investigations have demonstrated that such dendritic growth is not observed in Mg-based batteries.

Understanding the issues about interface stability and progressive morphological changes that take place during repeated cycles of stripping and deposition is one of the key aspects of developing better batteries. Lautar *et al.* [49] used DFT and KMC simulations to analyze the energetics and its impact on the growth mechanism on magnesium for different surface orientations to investigate the connection between the morphological evolution and surface orientation. They performed DFT calculations to estimate work functions, rate of surface adsorption, interaction energies, and energy barriers for diffusion, which they used as an input for KMC simulations of the diffusion processes. Their research demonstrates considerable variation in the energy barriers and, consequently, in the diffusion processes and morphological evolution for different surface orientations. Their findings support the idea that closely packed surfaces have lower surface energy than more open surfaces. They also discovered that higher adsorption is observed on less stable surfaces with weaker atomic coordination. They used the KMC simulations to study the surface dynamics as a function of relaxation time τ (the duration the system evolves to the relaxed configuration starting from an initial random configuration). Their results indicate the tendency of the deposition to exhibit epitaxial growth.

A rechargeable battery's charge and discharge rates are often constrained by the shuttled cation's diffusion coefficient between the electrodes. The identification of intercalation compounds with high guest cation mobilities has become a topic of interest since the structural and chemical properties of the electrode material highly impact cation diffusion coefficients. Spinel intercalation compounds are attractive materials for many metal-ion cell chemistry (Li, Na, and Mg). Kolli *et al.* [50] reported a thorough analysis of the diffusion of guest metal cations (*i.e.,* Li, Na, or Mg) inside these materials. A strong influence of concentration on the diffusion coefficient of cation was investigated using KMC simulations. In spinel compounds, guest metal cations favor octahedral sites, and they methodically explored cation transport in intercalation compounds within the face-centered cubic anion sublattice. They calculated cation diffusion coefficients using KMC simulations to determine the crystallographic and chemical causes for the substantial concentration dependency of diffusion coefficients of the cationic species in the spinel compounds. Their simulations showed that an intercalation compound's guest cation diffusion coefficient decreases sharply at intermediate-to-high concentrations of the cationic species, an undesirable property for batteries. They also found that the diffusion path of the cationic species within a host with a close-packed anion sublattice happens through a series of hopping mechanisms between octahedral and tetrahedral sites. This study uncovers important insights about diffusion within spinel compounds that may be very important in the design of electrodes with enhanced transport properties. Table 2 summarizes the research works using KMC for studying battery materials and their processes.

Table 2. *Summary of computational studies of Li and non-Li advanced batteries by KMC simulations*

Materials/systems	Computational tool	Highlighted features	Reference
Li-ion	KMC	Surface heterogeneity in graphite anodes	[51]
Li-metal (electrode)	KMC	Passive layer formation on metallic lithium anodes	[52]
Li-metal (electrode)	KMC- embedded atom technique	Effect of Li-atom deposition and its role onto the diffusion on the anode surface. Governing mechanisms under the operating condition and modification of the structural properties Li-anode	[48]
Li and Na mixed poly-anion solid electrolytes	KMC & GCMC	Enhanced Na-ion mobility in doped NASICON	[53]
Zn (electrode)	DFT & KMC	Aggregation of Zn during electro-deposition with Li^+ at the initial stage	[54]

Artificial intelligence and machine learning

Artificial intelligence (AI) and machine learning (ML) are the most important pillars of the fourth paradigm [55,56] in materials discovery. These tools leverage vast amounts of available data and algorithms to automate decision-making, uncover hidden patterns and relationships, and enable predictions and optimizations at much faster rates than previously possible. By incorporating these advanced technologies, materials scientists and engineers can discover new materials faster, predict their properties more accurately, and design and synthesize more efficient materials for diverse applications. A few examples of how ML can be leveraged are.

- Material property prediction: ML algorithms can be trained for the prediction of properties of new materials based on their chemical structure or composition, reducing the need for time-consuming and expensive experimentation [57-59].
- Automated discovery: ML algorithms can be used to systematically analyze very large amounts of data generated from experiments and simulations, identifying/designing new materials with desired properties more efficiently and accurately. AI & ML can also be used to design new materials with new properties by optimizing their chemical composition or structure [60-62].
- Material synthesis optimization: ML algorithms can be used to find optimal synthesis and processing conditions for materials to obtain desired properties, better yield and reduce waste [63,64].

In the context of batteries, ML and AI are being used to optimize and improve various aspects of battery design and production. For example, these technologies are invaluable in predicting the performance and stability of new battery materials [65,66], reducing the need for time-consuming and expensive experimentation. Additionally, ML algorithms can be used to analyze large amounts of data generated from battery testing and simulations [67], uncovering patterns and relationships that would be difficult or impossible to detect otherwise, thereby developing new materials with superior properties and improving the manufacturing process of batteries, production efficiency, and reducing costs. Overall, the integration of ML and AI in battery research and development enables faster, more accurate, and cost-effective material discovery and optimization.

Data-driven materials discovery and process optimization are indispensable tools for analyzing theoretical and experimental data. They establish essential structure-property relationships in materials. Current approaches in this direction typically combine high-throughput screening [68] and aim to identify new active electrodes and electrolyte materials for upcoming high-performance

batteries. ML techniques can be broadly classified into three categories: supervised, unsupervised, and reinforcement learning.

Supervised learning

Supervised learning techniques are the most used algorithms in battery research, particularly in materials discovery. Supervised approaches employ labeled datasets (inputs with corresponding outputs). Within the class of supervised ML, it is customary to differentiate between regression and classification. While classification bins the dataset in discrete classes. In contrast, regression is suitable for continuous values.

All ML algorithms intrinsically rely on data. Higher amounts of data lead to, in general, more accurate models. The data quality is an absolutely important factor since they might lead to misleading ML predictions (*e.g.,* problems caused by unreproducible data or error-infested data). Supervised ML algorithms map the input space to the output space by building a mathematical model that uses data to fine-tune the model parameters during training. One of the most prominent studies aimed to determine the factors influencing the high conductivity of the Li-ions in the solid oxide electrolytes having garnet-like structures (Kireeva *et al.* [69]). Solid electrolytes increase energy density by reviving the use of metallic Li anodes and alleviate much concern of liquid electrolytes typically used in commercial LIBs: toxicity, flammability, and limited electrochemical window. Their entire dataset, when combined with descriptors that encode information about the materials' production, had 168 compounds. To assess the Li-ion transport properties of the data and establish the composition-structure-ionic conductivity correlations, support vector machines (SVM) were employed in a regression analysis. Following that, the model was utilized to scan garnet-related structures for viable compositions and offer a bird's eye perspective of the solid electrolyte materials space, which is appealing for virtual screening, as shown in Figure 5.

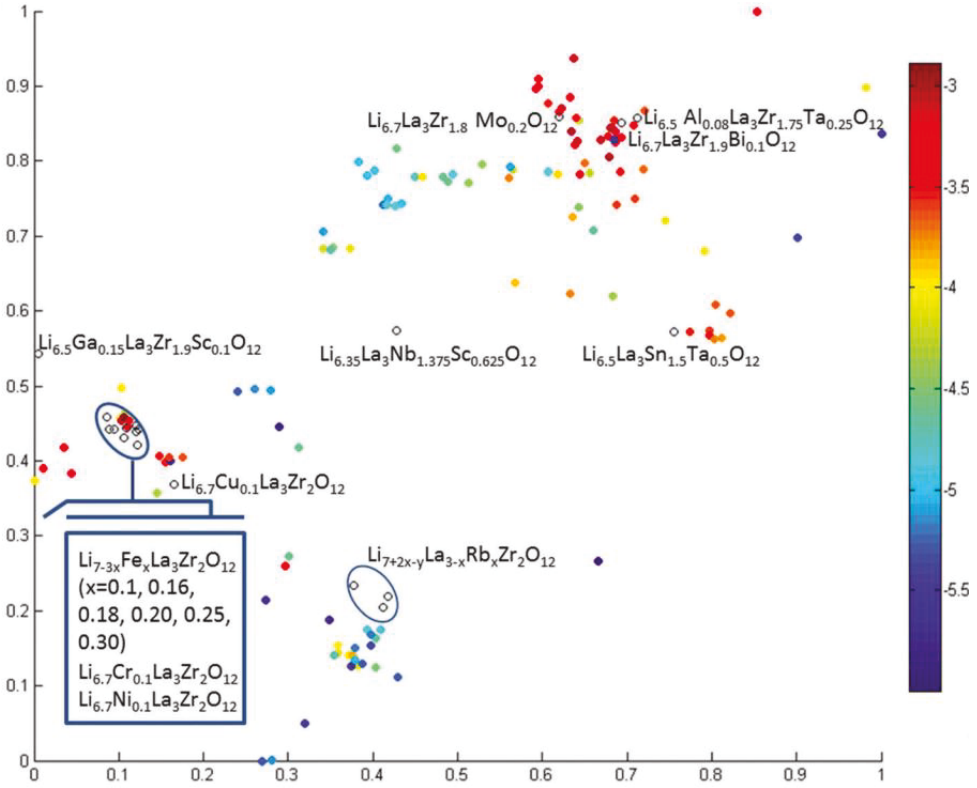

Figure 5. *Chemical space visualization displaying viable garnet-type materials with potential for application as solid electrolytes [69]. Copyright 2017. Reproduced with permission from RSC*

Manna *et al.* [70] used compositional factors inside ML tools to predict the specific capacity achievable for different potassium battery electrode materials. They employed various ML models: SVM, ExtraTrees Regression (EXR), and Kernel Ridge Regression (KRR). After considering 2118 data points of Li, Na, and K ion battery data from the Materials Project database [71] (of which 69.53 % are Li, 22.41 % are Na, and 8.06 % are K ion battery data) as the training set, they calculated the number of intercalated K ions inside the formula unit of the electrode by replacing the Li and Na with K based on the specific capacity values obtained. The stability of the intercalated electrode materials was then investigated using DFT simulations. Their findings demonstrate that ML algorithms can identify suitable electrode materials with high specific capacities without the high computational costs associated with DFT-based screening investigations, which is essential for effective battery technology.

Unsupervised learning

Even though supervised learning methods have been extensively applied in battery research, unsupervised learning methods have been relatively less explored. However, these algorithms provide us the opportunity to extract high-quality information about a battery system, with several automatically determined features that may provide deeper insight into battery performance.

Unsupervised ML algorithms use a dataset without labels and are tasked with clustering or associating the inputs. A clustering algorithm groups unlabeled data points into different groups based on their similarities and differences. The members of a group (or cluster) have the most similarity with each other. There are several clustering algorithms, such as K-means clustering, hierarchical clustering, and probabilistic clustering. On the other hand, association algorithms develop rules to find relationships between the points in a dataset. There are various association algorithms that exist, such as the Apriori algorithm, Eclat algorithm, and the Frequent Pattern (FP)-growth algorithm.

For solid-state lithium-ion conductors (SSLCs), Zhang *et al.* [72] used an unsupervised learning scheme and representation based on Bragg's law. This was used to map the three-dimensional (3D) periodic crystal lattice for the anion into a set of modified X-ray diffraction (mXRD), which was unique for the lattices of each anion. They represented 2986 compounds containing Li. They generated an unsupervised model using agglomerative hierarchical clustering and used them for grouping the mXRDs using a bottom-up approach for training. The model produced 7 groups and exhibited good quality clustering of known SSLC materials found using this scheme: with two clusters at the center having high room-temperature (RT) Li-ion conductivity (σ_{RT}) around 1 to 10 mS cm^{-1}. From the 2986 compounds that they started with, only 82 unique compounds were selected for MD simulations. Through the MD simulations, three new material systems, Li_8N_2Se, Li_6KBiO_6, and $Li_5P_2N_5$, were found to have a σ_{RT} exceeding 10 mS cm^{-1}, better than the best-known SSLCs. These new SSLCs comprise new structures and chemistries, showing unsupervised learning algorithms' power.

Chen *et al.* [73] used a novel end-to-end unsupervised ML scheme for more effective prediction of Na-ion battery life and failure using only the raw images of the charge-discharge voltage profiles. Li *et al.* [74] used an unsupervised data-driven technique to detect battery thermal anomaly by comparing the similarities in shape between thermal measurements. They clustered the measurements into groups based on their shape, and anomalies were detected by monitoring their deviations within the clusters. Their method was found to be more accurate than onboard battery management systems (BMS) and is also highly robust as it requires minimal reference data and is not affected by data loss.

Specific adaptation of computational approaches to battery chemistries

In LIBs, energy storage is essentially achieved through several chemical and electrochemical reactions, eventually making it possible to release the energy for later use. For optimization of such a system, different properties should be measured and considered as affecting parameters. However, all the ongoing reactions and occurring processes are not easily observable in a convenient way. Therefore, scientists have created several electrochemical models to detail the physical and chemical processes occurring in a battery to optimize its performance. These models strongly depend on the type of battery, materials, and design parameters of the system. In this part, we are going to discuss recent advances in the computational approach to better understand systems-level metrics of high-performing lithium batteries.

For the first time, in the 1970s, LIB was conceptualized and was commercially available around 1991 [75]. Generally, they consist of a graphite anode, separator, metal oxide cathode, and an electrolyte, a pathway for the lithium ions to go back and forth from the anode to the cathode through insertion chemistry [76]. A limited number of macroscopic variables, such as voltage (V), current (A), and temperature (T), can be measured in a non-destructive way and used in theoretical modeling. “Continuum models,” which consider physical characteristics to understand better the physicochemical processes such as Fick’s laws of diffusion, kinetics, and thermodynamic equations, are applied in a simplified way to simulate different aspects of a cell. Equivalent circuit models (ECM) are essentially a simplistic representation of a battery consisting of resistance and capacitors. In such a system, the underlying mechanisms of the electrode should be modified to a more comprehensive parameter until it satisfies the real experimental data [77]. By doing so, the state of health, state of the charge, or state of the capacity of the battery by the passage of time can be determined. For example, in a comprehensive study, four commonly used types of lithium-ion batteries, including lithium iron phosphate (LFP), lithium manganese oxide (LMO), lithium nickel manganese cobalt oxide (NMC), and lithium nickel cobalt aluminum oxide (NCA) is taken into account and the three types of equivalent circuit models (ECM), based on orders, (*e.g.,* first and second order ECMs) and a hybrid first-order ECM coupled with hysteresis are investigated to compare the accuracy of the result with real experimental data. They found that for LFP and NCA, the best-applied model is 1RC with hysteresis ECM, and for NMC and LMO, it was the 1RC ECM [78].

Monovalent (alkali) metal ion batteries

The first group column from the periodic table, except H, indicates alkali metals (AM). Among them, Li, Na, and K are considered here for alkali metal ion batteries because other alkali elements, such as Rb, Cs, and Fr, are rare/expensive/unstable elements. These elements contain a single electron in their last shell, which will be lost during the electrochemical reaction to give alkali metal ions. These ions then flow towards the cathode through an electrolyte and released electrons flow through the outer electronic circuit to cause an electric current. However, electrochemical reactions occurring in batteries involve multiple reactions, several physicochemical changes, and side products, which mostly downgrade the performance and capacity of the batteries over the period. Thus, understanding these reactions is necessary to overcome these issues.

Li-S battery

Researchers have intensively studied lithium-sulfur (Li-S) batteries due to their high energy density (2500 Wh kg^{-1}) and theoretical capacity of 1672 mAh g^{-1} [79,80]. A few problems, like the insulating nature of the sulfur element and its reduction product Li_2S, lead to low sulfur utilization. Moreover, during lithiation, the cell experiences a significant volume expansion, resulting in the

pulverization of active material sulfur [81]. To address those issues, computational approaches have been developed to study the reduction and oxidation reactions taking place in the battery.

One of the first mathematical models reported in lithium-sulfur was developed by Mikhaylik and Akridge [82]. A zero-dimensional model quantifies the polysulfide shuttle effect during charge and discharge. The model is based only on two-step reactions, the high plateau from S_8 to Li_2S_4 (419 mAh g^{-1}) and the lower plateau from Li_2S_4 to Li_2S_2 (837 mAh g^{-1}). This model accounts for heat generation because of the shuttle effect.

Similarly, Moy *et al.* [83] expanded the Nernst equations of Mikhaylik and Akridge's model by implementing intermediate reaction steps, Equations (1) to (6):

$$S_8 + 2e^- + 2Li^+ \leftrightarrow Li_2S_8 \quad (1)$$

$$3Li_2S_8 + 2e^- + 2Li^+ \leftrightarrow 4Li_2S_6 \quad (2)$$

$$2Li_2S_6 + 2e^- + 2Li^+ \leftrightarrow 3Li_2S_4 \quad (3)$$

$$Li_2S_4 + 2e^- + 2Li^+ \leftrightarrow 2Li_2S_2 \quad (4)$$

$$Li_2S_4 + 6e^- + 6Li^+ \leftrightarrow 4Li_2S \quad (5)$$

$$Li_2S_2 + 2e^- + 2Li^+ \leftrightarrow 2Li_2S \quad (6)$$

The objective of this model was to measure the shuttle effect rates and predict capacity fade. However, the model calculates the rate of the shuttle by holding the cell at a constant voltage, which limits its application.

Kumaresan *et al.* [84] developed a one-dimensional model for Li-S batteries. Along with time evolution and spatial distribution of polysulfide precipitates, the impact of variations in the separators and cathode's porosity is also considered by Kumaresan's model. Therefore, the Kumaresan model is helpful as it provides a simple yet accurate way of predicting the behavior of lithium-sulfur batteries. It can be used to design better battery management systems and optimize these batteries' performance in real-world applications. However, like all mathematical models, it has its limitations, as it only considers the transport of lithium ions through the electrolyte in one direction (*i.e.,* from the anode to the cathode). This simplification allows the model to be solved more efficiently and quickly. Still, it also means that the model may not be as accurate as more complex models that consider the transport of lithium ions during the charging process.

A similar model was created by Neidhardt *et al.,* which simulates the precipitation of polysulfides at various solid-liquid interfaces [85]. This model tracked the interactions between sulfur and electrolyte, carbon electrolyte, and precipitate and electrolyte separately. Instead of utilizing the Butler-Volmer kinetics approach, the researchers employed potential-dependent mass action kinetics to describe the rate of electrochemical reactions. Using this framework, they created a 1D model that could predict the charge-discharge voltage curves and impedance spectra.

The findings suggested that the presence of solid phases (product and reactant) in interaction with dissolved anionic polysulfides influences the discharge performance of a lithium-sulfur cell. Furthermore, the model predicted an uneven phase formation and dissolution behavior during cell cycling (charging and discharging) and higher over-potentials.

Marinescu and coworkers developed a zero-dimensional model for predicting the behavior of a lithium-sulfur cell during charging and discharging [86]. The model considers two electrochemical reactions through the mathematical formulation of the Nernst equation, Butler-Volmer kinetics dictated power limitations, and precipitation/dissolution of chemical species [87]. The model shows that the low-voltage plateau's flat shape, typical in the discharge of a lithium-sulfur cell, is caused

by precipitation. On the other hand, during charge, the model predicts that dissolution can act as a bottleneck, limiting the amount that can dissolve at large currents.

Li-Si battery

Silicon is one of the most promising anode materials for Li-ion batteries owing to several advantages such as high specific capacity, its high abundance (28 %, second most among all elements; oxygen being first at 47% on a mass basis) in an earth's crust, and its low cost. Despite many advantages, commercialization of silicon-based Li-ion batteries is hindered due to key issues like high volume expansion during charging and discharging and its innate poor electrical conductivity [88,89]. To overcome these issues, many approaches, such as the use of nanocomposite Si [90,91], and the use of morphologically modified nanostructures such as porous Si [92-94], Si nanowires [95], core-shell structures [96,97], hollow nanoparticles [98,99] are reported to date. However, obtaining ultrafast chargeable and long-term stable Si anode material is still challenging. The main challenge arises during the intercalation process [89] when the silicon anode experiences a large volume expansion 300 % owing to a large intake of Li per Si atom. Such a huge volume expansion creates enormous stress on its structure and leads to mechanical failure/fracture. This further causes electrolyte decomposition by providing direct contact with the Si anode and electrolyte.

Chan *et al.* [101] and Jung *et al.* [102] showed that the process of lithiation and delithiation of crystalline Si is anisotropic and favors (110) surface over (100) and (111) surfaces due to its small interfacial energy at the interface of amorphous Li_xSi/crystalline Si. This promotes lithiation behind the interface and causes volume expansion along <110>. The amorphization process of Si and diffusion of Li ions during cycling plays an important role in the performance of the Si anode. Pan *et al.* calculated the average coordination number (CN) for the interaction of Li ions in amorphous Si and suggested that stress can increase Li ion diffusion either by increasing free volume under tension or by changing local structure during compression [103]. Choi *et al.* [100] found that Li-ion diffusion in c-Si follows tortuous diffusion pathways and the degree of the tortuosity varies with the orientation of Si. Thus, Li-ion diffusion through Si<110> tends to take a less winding path to move a particular distance when compared with diffusion through Si<111>. The Li ions diffusion pathway that migrates through the different lattices is shown in Figure 6.

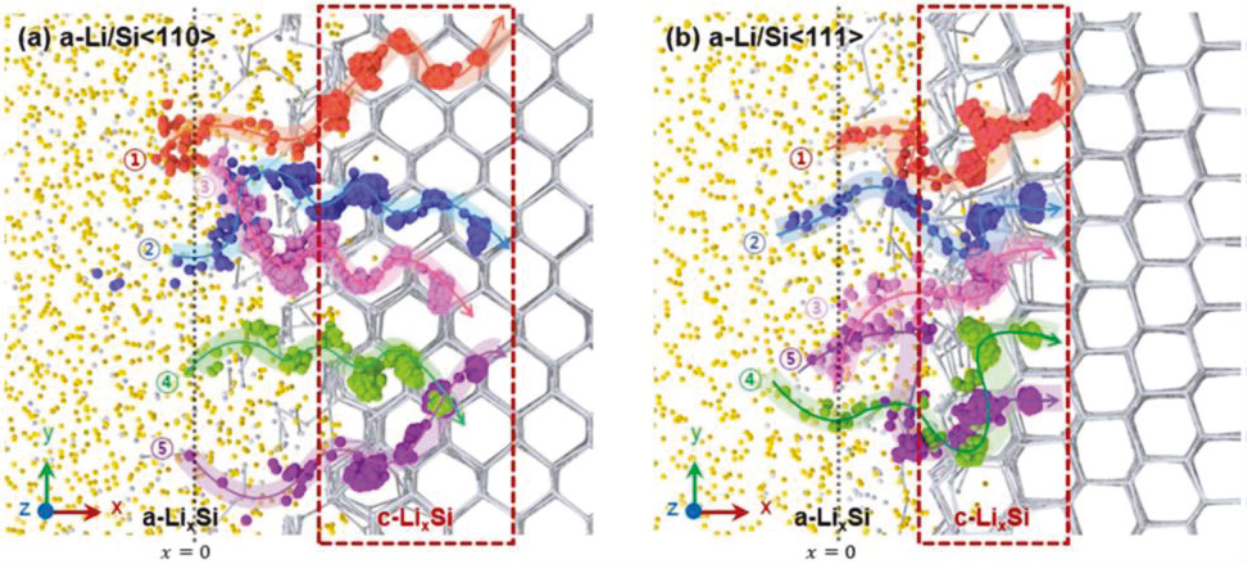

Figure 6. *Magnified views of Li diffusion at the interfacial region of the (a) a-Li/Si<110> and (b) a-Li/Si<111> diffusion couples [100]*
Copyright 2017. Reproduced with permission from Springer Nature

The interface of Si/Li_xSi plays a crucial role in volume expansion and studying the factors affecting its nature and mechanical strain distribution during the lithiation process will be beneficial to alleviate pulverization of Si anode. Wang *et al.* [104] showed that the presence of LiF on Li_xSi at x>1 leads to the formation of delocalized stable voids, which allows the interface structure to deform plastically. However, tightly bonded Li_2O to Li_xSi is stiffer and causes rigid deformation across all x. Thus, the presence of a higher amount of LiF enhances the ductility of the SEI layer.

Jiang *et al.* [105] carried out quantitative analysis by proposing a zero-dimensional mechanistic model of Si anodes for LIBs and showed that a slower crystallization rate leads to the abrupt exponential growth of crystalline silicon, while increased crystallization rate gives a sigmoidal profile. Figure 7 (a) shows the different voltage curves. Figure 7 (b) depicts that the sufficient increase in the surface energy barrier (E^*) causes the elimination of higher voltage peaks from the differential analysis of Si anode and, therefore, other techniques will be necessary to analyze Li-Si chemistry. In addition, Figure (7 (c) and (d)) indicates the variation in the growth rate of crystalline and amorphous phases of Li-Si composition with the increment of surface barrier energy. These results confirmed the important role of higher surface barrier energy behind the poor performance of bulk Si anode compared to Si nanoparticles.

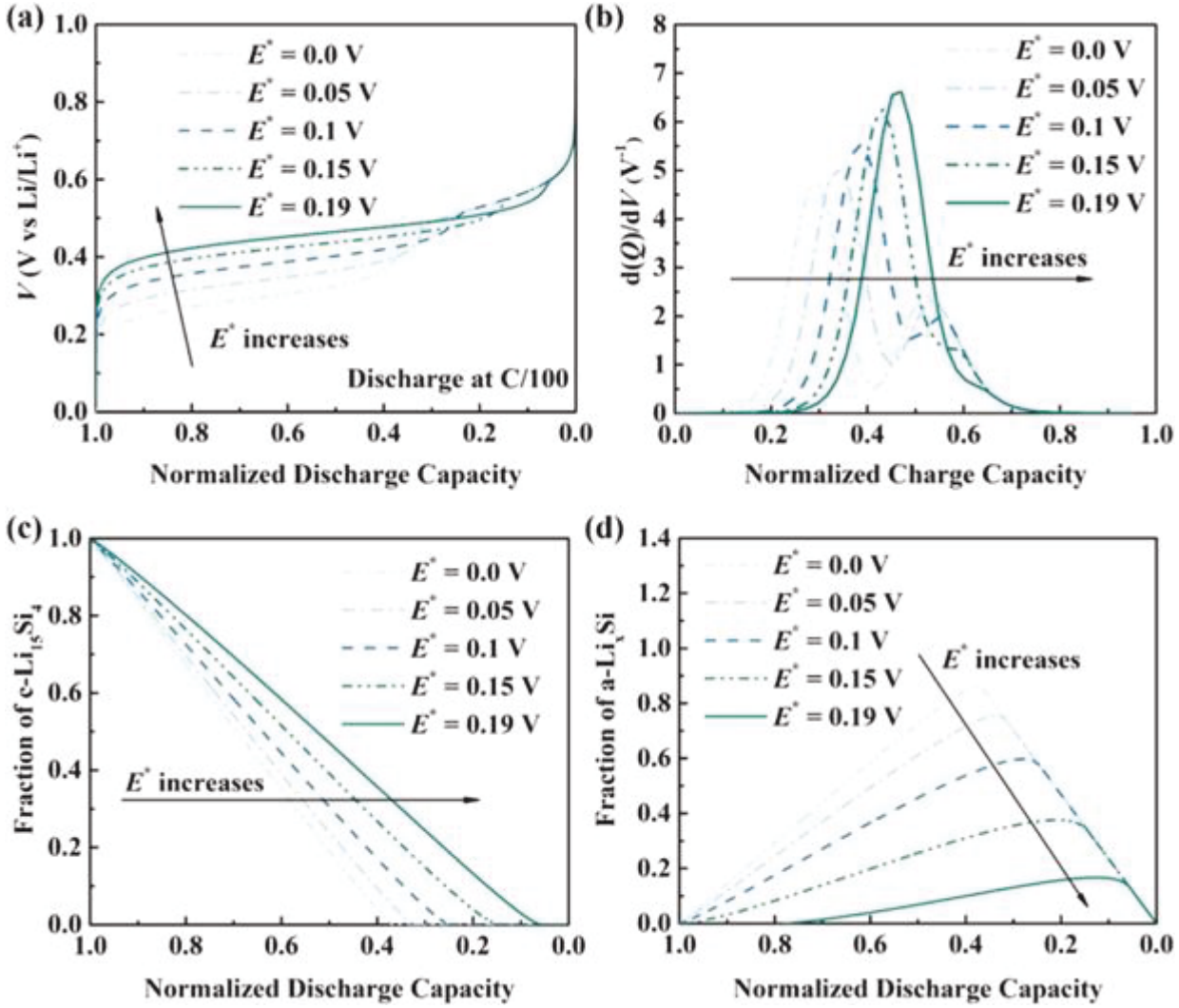

Figure 7. *(a) Voltage curves, (b) differential voltage curves, and molar fraction variation of (c) c-$Li_{15}Si_4$, and (d) a-Li_xSi at different values of surface energy barrier during discharge [105]*
Copyright 2020 Reproduced with permission from IOP Publishing Limited

Damle *et al.* [106] studied the structural stability of Si-CNT heterostructure as a function of Si configurations using the finite element method (FEM) and found that Si droplets configuration is more stable than continuous Si coating configuration due to reduced mechanical constraints. In another study, Dhillon *et al.* [107] used FEM to study a porous silicon-graphite composite electrode and found that at lower reaction rates, the electrode with high initial porosity is fully utilized prior to reaching cut-off potential. A comparison of the computational results with experimental observations revealed that the main reason for capacity fade is the increase in tortuosity in the diffusion pathway of lithium ions due to cracking of the silicon composite electrode upon electrochemical cycling. An experimental approach to enhance the electrical conductivity and mechanical stability of Si-composite anode was explored by Suh *et al.* [108], who used Co to obtain $Si/SiO_x/Co$ composite anode, which performed much better than pure Si due to good electrical and ductile property of Co. Surface coating is another strategy to provide additional mechanical stability to the Si anode which can avoid pulverization of Si by providing Li diffusion through an extra layer, and thus enhancement in the cyclic performance of the Si anode [109]. However, obtaining a thin and stable coating is challenging as the chemical composition and mechanical properties of this coating change during the cycling process. Kim *et al.* [110] constructed a reactive force field (ReaxFF) parameters to simulate the lithiation process for Si/Al_2O_3 and Si/SiO_2 nanostructures and correlated the chemical and mechanical changes during lithiation and delithiation.

They found an elastic modulus gradient created due to self-accelerating Li diffusion across Al_2O_3 coating, which eliminates local stress concentration and crack propagation through Si electrodes. Gao *et al.* [111] used MD simulation to study alumina-coated Si nanowires (SiNWs) and suggested metal oxide-coated SiNWs ductility improved from 16 % to greater than 47 % without any reduction in the tensile strength. The enhancement during the lithiation process is caused by the absorption of strain energy from metal oxide to assist volume expansion and by increasing the rate of defect nucleation from the core-coating interface to prevent localized deformation. Shaung *et al.* [112], by performing large-scale atomistic simulations, successfully capture structural changes and volume expansion, which experimentally occurs on maximum lithiation of SiNPs, hollow a-SiNPs, and solid crystalline SiNPs. The authors found that the hollow a-SiNP has the highest fracture resistance and hence, it is the best configuration of Si to use as an anode for LIBs.

Since electrical conductivity and mechanical stability are important properties of electrode materials, obtaining atomically thin 2D nanolayers as anode is more beneficial due to excellent electrical conductivity and mechanical robustness [113,114]. Silicene, a thin nanolayer of Si, is one the best anode materials owing to key advantages such as enough space for adsorption/migration of Li ions during the cycling process, low volume expansion, high mechanical strength and small diffusion energy barrier [115]. However, obtaining pristine flat Silicene is still challenging today as, unlike graphene, the radius of the Si is 1.8 times larger than that of C, which distorts the planar structure of the silicene and high reactivity of Si with O, which readily forms Si-O bond. To obtain a stable silicene structure, several strategies, such as the use of 2D/2D heterostructures [116], doping on silicene [117] and a few layered silicenes [118], have been proposed as anode for LIBs. Momeni *et al.* [119] used DFT to calculate Li adsorption energies and diffusion characteristics on doped silicene. Doping of silicene with B, N and P significantly increases adsorption energy, indicating higher Li storage. Further, N and P-doped silicene have lower surface diffusion barrier energy, while Al-doped has a lower vertical diffusion energy barrier. Galashev *et al.* [120] conducted an MD study to explore the cycling process of a bilayer of silicene-based anode on Cu substrate and the effect of vacancy-type defects on its performance. They found vacancy defects larger than bivacancy reduce the mechanical strength of

the silicene sheet, which ultimately increases deformation. Ipaves *et al.* [121] studied Al functionalized trilayer silicene by considering the thermodynamic stability of ABC-Si_4Al_2 for alkali metal ion batteries with AIMD simulations. Results suggest that diffusion barrier energy is like that of graphite, with an average OCV ranging from 0.14 to 0.49 V along with a high capacity of 645 mAh g^{-1} for $Li_4Si_4Al_2$. In another study, Galashev *et al.* [122] found that vertical intercalation processes had smoother total energy change than horizontal intercalation. Rehman *et al.* [123] studied the anodic properties of hydrogenated silicene for the application of Li and Na-ion batteries. Based on PBE and HSE06 schemes, silicene showed a semiconducting nature with indirect bandgap and excellent adsorption strength. The diffusion barrier energies for Li and Na ions were 0.18 and 0.14 eV, indicating ultrafast diffusion channels and an average open circuit voltage of 0.42 and 0.64 V, respectively. With advantages such as enough adsorption/migration of Li ions, low volume expansion, high mechanical strength, and a small diffusion energy barrier, silicene is the best anode material for LIBs.

Na-ion battery

Li-ion batteries have been the most dominant player in the energy storage market for the last three decades due to their robust electrochemistry and high storage capacity. However, the increasing demands of energy storage devices, lack of Li resources and geopolitical distribution of Li salts are major concerns diverting materials scientists to consider an alternate option for Li. Sodium (Na) ion battery (SIB) is one of the best options to replace Li-dominated energy storage devices owing to several advantages. Firstly, sodium resources are abundant and available globally at low prices. Secondly, SIB chemistry is almost like that of LIB and hence, major changes on the production line will not be required. Compared with Li-ion, Na ion has a larger ionic radius, higher standard electrode potential vs. standard hydrogen electrode (SHE) and lower melting point [124]. As a result, phase behavior, diffusion coefficients and chemistry at the electrode-electrolyte interface significantly change for SIBs [125]. In addition to understanding Na-ion chemistry, the performance of the SIBs must not be limited to a narrow range of temperatures. The poor performance of SIBs at low temperatures is associated with sluggish electrochemical reaction kinetics, which causes unstable interfacial reactions [126]. Thus, to obtain SIBs with high capacity, it is necessary to find appropriate electrode materials with smooth Na-ion diffusion, good reaction kinetics and excellent thermal as well as chemical stability. The similarity in the chemistry of Li and Na allows the implementation of advanced strategies from LIBs to SIBs.

As 2D nanomaterials can show high carrier mobility, good electrical and thermal conductivity, and excellent mechanical stability, most recent studies focus on designing new 2D nanomaterials. Recently, Gu *et al.* [127] studied 2D transition metal compounds to enhance the specific charge capacity of LIBs. Inspired by this study, Banerjee *et al.* [128] studied six Co-based anti-MXene (CoAs, CoB, CoP, CoS, CoSe, and CoSi) materials as potential anodes for SIBs. Authors report all these six Co-anti-MXenes to possess high specific capacity (390-590 mAh g^{-1}), greater affinity, low average sodiation potential and smaller diffusion barrier energies. Wei *et al.* [129] studied a 2D vanadium boride (V_2B_2) as an anode for SIBs by using first principles. Their study showed V_2B_2 can adsorb 3 layers of Na ions so that its capacity can reach a maximum of 814 mAh g^{-1}. Further, its ability to maintain metallicity throughout the sodiation process indicates good conductivity and a very low diffusion barrier energy of 0.011 eV indicates an ultrahigh diffusion rate, which is necessary for high-capacity batteries for vehicles. Moalla *et al.* [130] used DFT calculations to verify the application of a graphyne-like BN layer (BN-yne) as anode for SIBs. Authors suggested BN-yene accumulates maximum Na ion with $Na_4B_2N_2$ configuration and cell voltage was found to increase from 1.70 to

2.10 eV under the influence of an electric field of -0.02 a.u. In another DFT study, Ye *et al.* [131] considered a 2D monolayer of C_3N as anode for SIBs. Authors computed maximum theoretical capacity of C_3N to be 543.89 mAh g^{-1} with low activation energy barrier of 0.112 eV and low average OCV of 0.83 V. Li *et al.* [132] used DFT calculations to study three composition of titanium zirconium metal carbides ($TiZrCO_2$, $Ti_2ZrC_2O_2$, and $TiZr_2C_2O_2$) for potential application as an anode for SIBs. Their study showed all these three compositions store a double layer of Na on each layer and exhibit good capacities of 586, 441 and 375 mAh g^{-1}, respectively.

The potential application of Si as an anode for SIBs is found to be efficient only in the presence of some additives or with graphene-based interlayers. To understand the role of the Si/graphene interface for SIBs, Raghuvanshi *et al.* [133] investigated the Si/graphene interface using first-principles calculations along with experimental results. They found the most stable position for Na ions in the Na-Si-graphene system is at the Si/graphene interface, where electrons transfer from Na to C and cause C to be more electronegative when compared with Si. The presence of a high concentration of Na at the Si/graphene interface is verified by depth profiling ToF-SIMS and thus validates the reason for an increase in the Na storage for the Na-Si/graphene system. Obeid *et al.* [134] considered the 3D network of 2D biphenylene nanoribbons as an anode for SIBs using DFT and MD. They found the presence of p_z-orbitals (π-bonds) on sp^2 carbon atoms throughout the network leads to excellent metallic nature. HexC28 can deliver specific gravimetric and volumetric capacities of 956 and 1109 mAh mL^{-1}, respectively, with little volume change and a lower diffusion barrier. Zhou *et al.* [135] used first-principles calculations to study the properties of haeckelite hexagonal monolayer as an anode for SIBs. The presence of a large radius heptagon causes smooth Na ion adsorption on the monolayer with a low diffusion barrier of 0.30 eV. The calculated storage capacity is 116.71 mAh g^{-1} with a small open circuit voltage of 0.37-0.16 V.

The presence of defects in the structure can change the electronic properties of the materials. Therefore, to study the properties of defected graphene quantum dots (dGQDs) as anodes for SIBs, Daryabari *et al.* [136] used DFT calculations. Authors considered the interaction of Na atom/ion with various defects such as F_3.Gr, F_3H_3.Gr, N_3.Gr and N_3H_3.Gr and suggested that the extent of charge transfers between Na atom/ion and dGQDs varies with elements at the defect site. Additionally, they suggested that F-doped defects deliver cell voltages of 1.54-1.58 V, which is higher than that of N-doped defects having cell voltage of 0.58-0.61 V.

Obtaining high-voltage stable cathode materials for SIBs is equally important as charge storage capacity and the final potential difference between the anode and cathode signifies the energy density of the battery. Unlike LIBs, where the presence of Co is essential for good performance of cathode materials like CoO_2, cathodes for Na-ion batteries can be made without use of Co and thus can be cost-effective. Chu *et al.* [137] provided a comprehensive summary of the experimental study of Co-free cathode materials for SIBs.

Phosphate-based cathodes are more favorable for SIBs due to their high structural stability. To understand the Na-ion transport mechanism and important properties of vanadium phosphate cathode materials, Aparicio *et al.* [138] used DFT calculations along with MD. Authors reported that Na ion mobility is highest for α_I-$NaVOPO_4$ polymorphs with the least activation energy of 0.32 eV when compared with α-, β- NaVOPO4 polymorphs with activation energies of 0.35 and 0.51 eV, respectively. Further, partial doping of vanadium with other metals significantly increased the cell potential of α-, β- NaVOPO4 polymorphs compared to α_I-$NaVOPO_4$ polymorph. Due to stability and high electrode potentials, the manganese-based NAtrium SuperIonic CONductor (NASICON) type phosphate framework is most favored for “rocking chair” batteries. Snarskis *et al.* [139] used DFT,

cluster expansion and semi-grand canonical MC methods to study the thermodynamics and phase formation of NASICON-type $Na_{1+2x}Mn_xTi_{2-x}(PO_4)_3$ ($0.0 \leq x \leq 1.5$) electrode materials for SIBs. Their results indicate the existence of three phases, stoichiometric $Na_3MnTi(PO_4)_3$, $NaTi_2(PO_4)_3$ for $x < 1.0$ and $NaMnPO_4$ for $x > 1.0$ at all temperatures. Additionally, the presence of a strong anti-bonding character and strong hybridization between Mn(3d)-O(2p) makes it a weaker bond than the Ti-O bond, which governs Mn-based NASICONs stability.

Gurmesa *et al.* [140] used first-principles calculations to study Na_2MnSiO_4 structure under the influence of biaxial tensile and compressive strain. The author suggested changes in band gap energy with respect to applied biaxial tensile strain or compressive strain, indicating strong coupling of the p-d(σ) bond for the O-Mn bond. Moreover, tensile strain causes a reduction in activation energy and, hence, enhancement in Na ion diffusivity, which is beneficial for fast rechargeable SIBs.

Peng *et al.* [141] carried out the experimental and computational study of Al^{3+} doping in O^{3-} type layered $NaNi_{0.5}Mn_{0.5}O_2$ cathode material. Authors reported an enhancement in the retention capacity of electrode material as Al^{3+} doping leads to reinforcement of metal-oxygen bonds and reduction in diffusion barrier energy for Na ion. The calculated energy density for a full cell with commercial hard carbon was 213.5 Wh kg^{-1}.

K-ion battery

Potassium (K) ion batteries (KIBs) are another alternative option to replace LIBs due to several advantages: enhancement of K-ion diffusion through solvents as smaller stokes radius, cost-effective as Al can be used as a current collector, and the possibility of high voltage battery [142-144]. Despite these advantages, the large ionic radius of K-ion causes poor performance with low capacity, poor rate performance and fast capacity decay over time [145]. Additionally, compared with Li and Na, the high molar mass of K significantly reduces the energy density of the KIBs. With the use of computational and experimental techniques to overcome challenges associated with KIBs, it is necessary to understand the failure mechanism and chemistry of K-ion with current electrode materials so that further chemical and structural modifications can be applied to obtain superior electrode materials. Additionally, considering various computational techniques and modeling, potentially stable and robust electrode materials can be found for KIBs.

Chengxi Zhao *et al.* [146] examined the nitrogen (N)-doped CNTs (N-CNT) and the effect of tubular size on the adsorption capabilities of Li^+ and K^+ at the doping site and their penetration. A comprehensive investigation of the adsorption complexes' electronic structures, adsorption energies, and minimum-energy routes for alkali metals (AM) migration through these defects was performed using DFT. They believe that the pyrrolic-N defects perform better than the pyridinic counterparts in Li^+ and K^+ battery systems, allowing easier passageways of Li^+ and K^+ through these defects. This is the opposite in graphene-based systems where the pyridinic defects are better than pyrrolic ones [147]. Their studies proved that the curved walls of N-CNT favor the pyrrolic defect. In CNT-based metal ion batteries, both external and internal CNT surfaces participate in Li and K ion storage, with the former playing a larger role in the performance. As mentioned earlier, N-doping is a widely accepted approach to improve the AM-CNT binding affinities, henceforth enlightening the battery performance. In this study, Li and K ion binding with 3 types of N-doping sites named graphitic-, pyridinic, pyrrolic- in three different tube sizes: (8,0), (10,0), and (12,0) is explained in Figure 8. This study paves a path for improving battery performance metrics [146].

Yu *et al.* [148] used high throughput computational screenings to study and explore the multiple KIBs anode materials. The Material Project database was used to study the conversion and alloying

reactions of KIB anode materials. For the theoretical capacity and reaction potential calculations, they use the grand potential diagrams. From their Material Project database calculations, they concluded that the Si, Sb P, and As anodes showed high capacities.

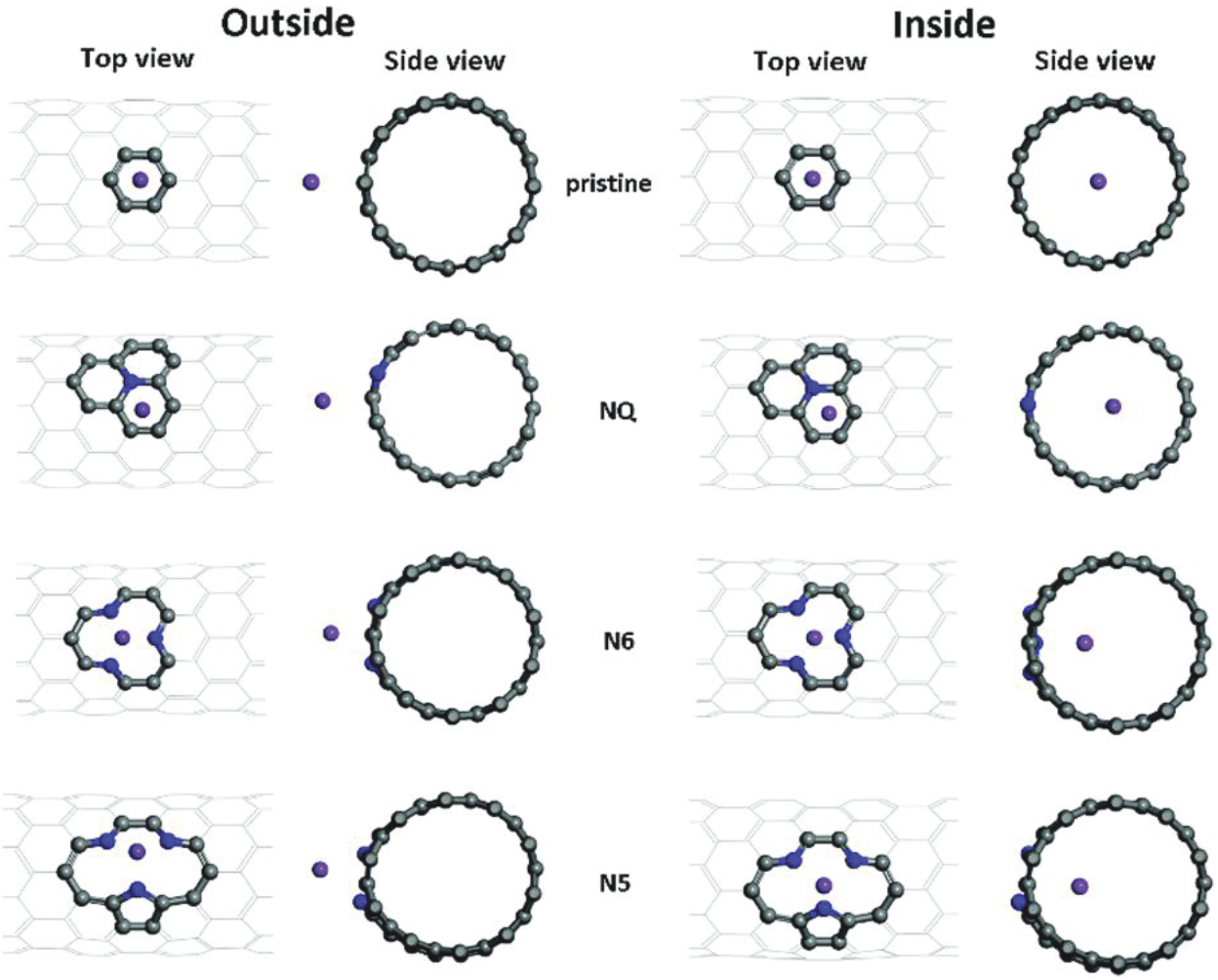

Figure 8. *Different adsorption configurations of K/Li on pristine, NQ, N6 and N5 CNTs. Shown here are the optimized adsorption complexes for the K atom on (10, 0) CNTs [146]*
Copyright 2019, Reproduced with permission from RSC

Additionally, their results confirmed that the phosphides usually display a comparatively inferior reaction potential compared to oxides and sulfides. There are eighteen binary compounds that showed low reaction potential and high theoretical capacity (0.7 V, greater than 450 mAh g^{-1}, respectively) that were thought of as promising KIBs anode materials. In specific, V_3S_4, CuP_2, ZnP_2, NiP_3, SiP, Nb_3S_5, CoP_3, Ga_2O_3 Bi_2O_3, showed high theoretical capacities. The reaction potential and theoretical capacities are shown in Figure 9. The alloy-type compounds P, Sb, Bi As, Si, and Ge showed higher capacities than the conventional graphite (C) anodes. Screening helped to identify eighteen binary compounds (four oxides, six sulfides, and eight phosphides) with high capacity and lower reaction potential. Amongst these phosphides, higher capacities were observed for SiP CuP_2 and ZnP_2 (681, 712 and 842 mAh g^{-1}) with average potentials of 0.60, 0.50 and 0.51 V, respectively. In the case of sulfides, Nb_3S_5 and V_3S_4 exhibited capacities of 611 and 763 mAh g^{-1} with average potentials of 0.69 and 0.61 V, correspondingly. Among the oxides, Ga_2O_3 and Bi_2O_3 showed high theoretical capacities of 690 and 524 mAh g^{-1}, respectively. Usually, the alloy-type material with high theoretical capacities showed unusually high-volume expansion to the tune of 200 to 600 %, which could result in capacity degradation during continuous charging-discharging cycles. Consequently, volume expansion control

buffering matrices like CNTs, MOFs, and COFs may be implemented to prevent these excessive volume changes [88] or the anode materials having reasonable theoretical capacities with little volume expansion need to be explored [148].

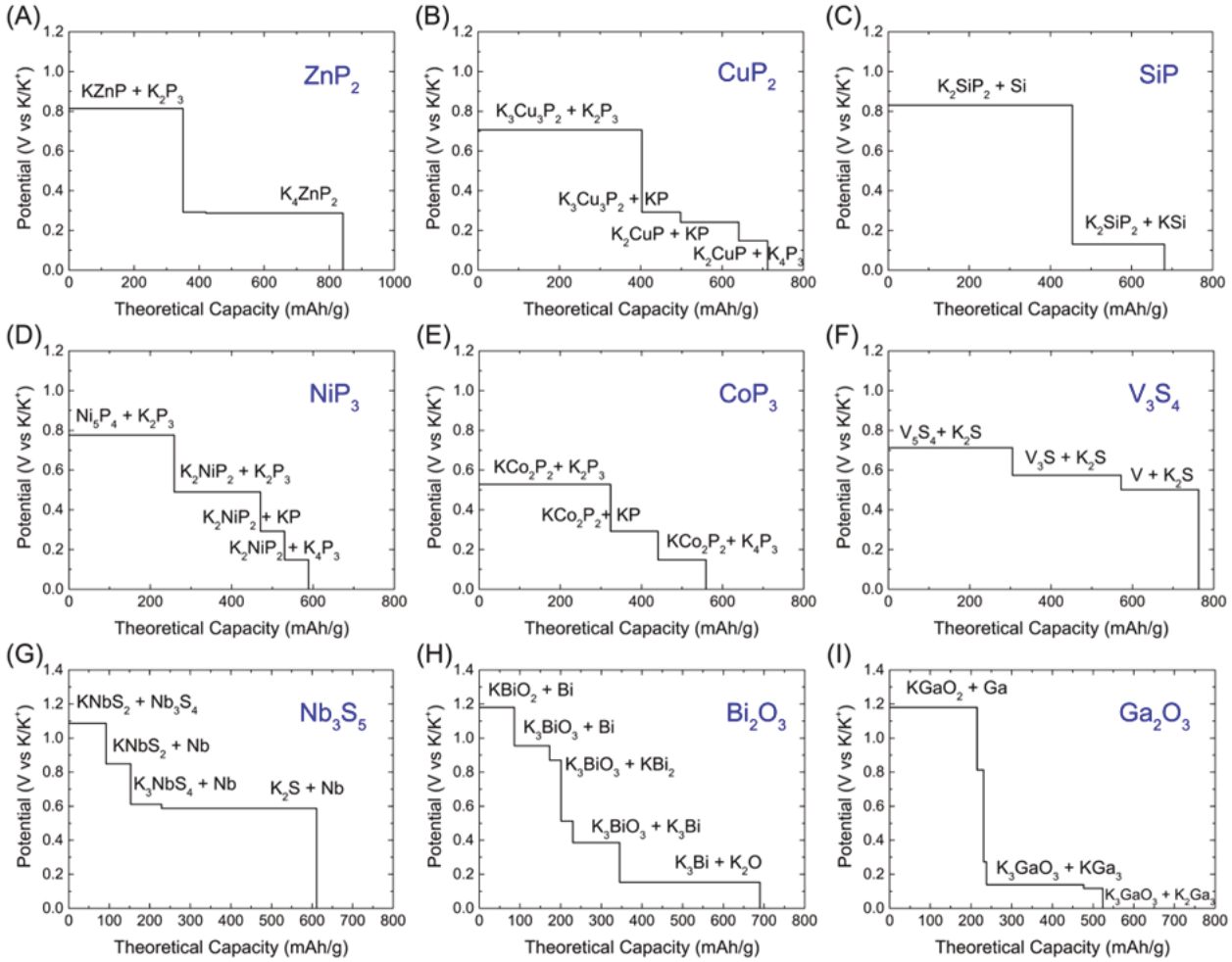

Figure 9. *Potassium ion battery anodes (PIBs): reaction potentials and theoretical capacities of binary compounds: A, ZnP_2; B, CuP_2; C, SiP; D, NiP_3; E, CoP_3; F, V_3S_4; G, Nb_3S_5; H, Bi_2O_3; and I, Ga_2O_3 [148] Copyright 2019. Reproduced with permission John Wiley and Sons*

Multivalent metal-ion batteries

Cost reduction and increased power densities are crucial to the growing market acceptance (like in EV technologies). The alkali metal ion (monovalent) batteries, *e.g.,* lithium and sodium, have become a mainstay for current energy storage devices due to their high-power density, longer cycle life, and good rechargeability. However, they have some critical downsides, such as safety issues, reliability, and high cost. There is an urgent need for potential alternatives that can fulfill the requirements of improved safety, lower cost, better sustainability, and natural profusion. Multivalent ion (Al^{3+}, Ca^{2+}, Mg^{2+}, and Zn^{2+}) batteries, which consist of an intercalation cathode and a multivalent metal anode, have recently gained extensive research interests because of their low cost (huge natural abundance) and better capacity. The comparison between capacities (both gravimetric and volumetric) and the natural abundance of different battery systems are shown in Figure 10.

The key factor for material modeling is to explore the nature of processes occurring during the charge-discharge cycles, which is directly related to the ionic diffusion of electrode and electrolyte materials. MD simulation is one of the most feasible approaches to determine the ionic diffusion of the materials. OCV is equally important and can be optimized using electronic structure calculation.

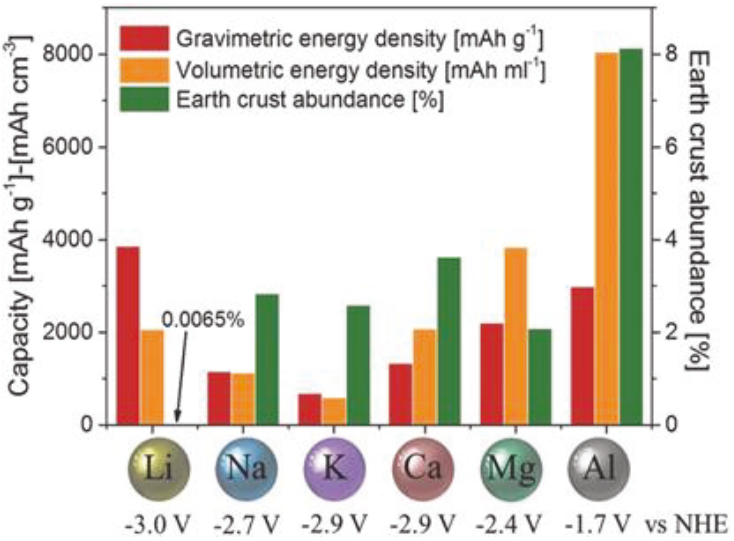

Figure 10. *Comparison between volumetric and gravimetric capacities, standard reduction potential Vs NHE, and natural abundance of different metal electrodes used for battery application [149]*
Copyright 2016, reproduced with permission from John Wiley and Sons

To find out the cost-effective and promising material for multivalent-ion batteries, several theoretical investigations have been performed in recent years [150]. The layered compounds in the Materials Project database were screened and DFT calculations were performed by Zhang *et al*. [151], resulting in over 20 distinct types of promising candidate materials as cathode for multivalent batteries. The flowchart is also shown in Figure 11.

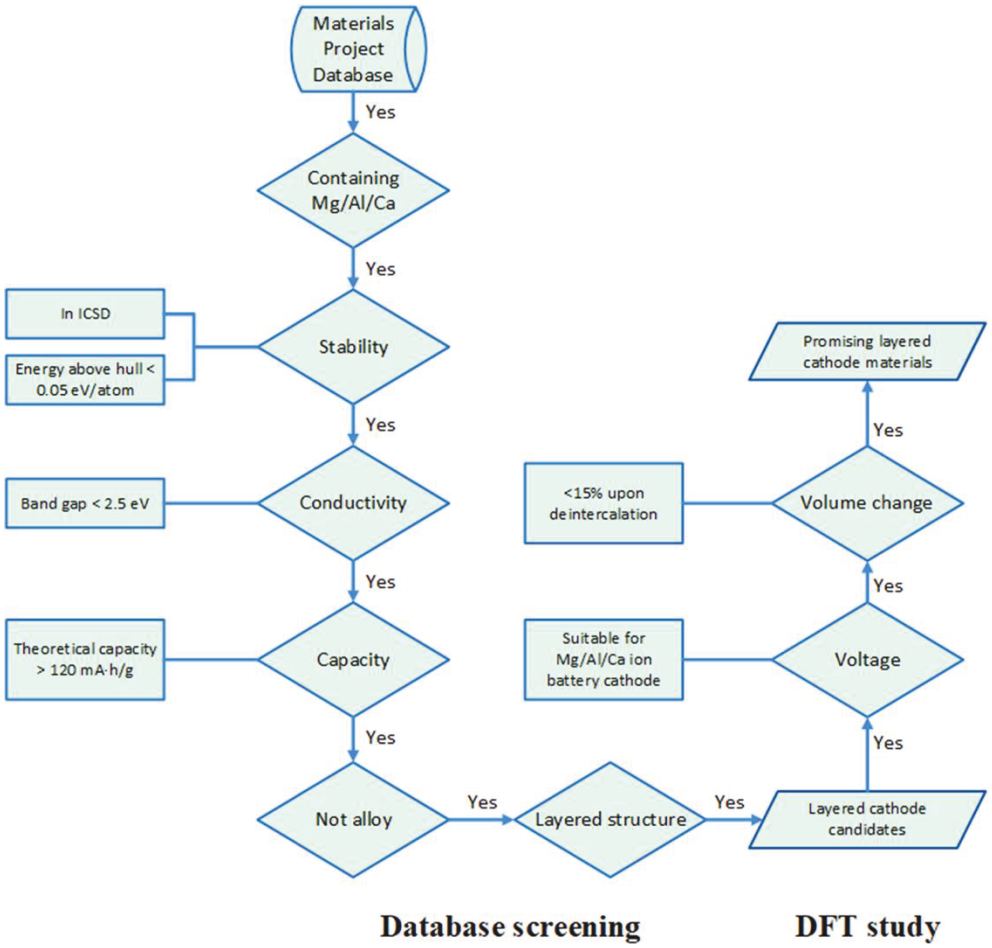

Figure 11. *Flowchart for the screening process for promising multivalent cathode materials [151]*
Copyright 2019, reproduced with permission from ACS publication

In the following subsections, we will discuss the computational approaches for aluminum-ion batteries (AIBs), magnesium-ion batteries (MIBs) and zinc-ion batteries (ZIBs) separately.

Aluminum-ion battery

To identify promising electrode materials for aluminum-ion batteries (AIBs), theoretical research based on first-principles simulations within DFT formalism has gained interest in recent years. Pal *et al.* [150] did a thorough review of the performance and mechanical understanding of AIBs in the post-LIB arena. The kinetics of Al insertion into alpha-MnO_2, a potential cathode for AIB, have been predicted using the climbing-image nudge elastic band (C-NEB) approach by Alfaruqi *et al.* [152]. To comprehend the underlying rationale for the usage of the graphite cathode for enhancing performance of AIBs, several computational experiments using DFT have been investigated by Li *et al.* [153]. Theoretical investigation of the crystal structure through first-principles calculations and the intercalation- deintercalation mechanism of Al ions in the AIBs were carried out by Wang *et al.* [154]. In this battery system, long cycle life, low cost, and good capacity are attained. After 100 cycles, the discharge capacity is still 116 mAh g^{-1} at a current density of 50 mA g^{-1}. The multi-valent battery can store a large number of charges and increase specific capacity in comparison to monovalent batteries.

Magnesium-ion battery

Magnesium has limited ductility due to its hexagonal crystal structure. The brittle characteristic of magnesium is a significant barrier to overcome in fabricating suitable thin foils for anodes in batteries. By adding modest amounts of doping elements, Mg's ductility can be improved. To reduce Mg brittleness, Vincent *et al.* [155] did a computational screening of 34 known dopants for Mg. It is important to know which of them are stable in bulk without modifying the electrochemical properties, and it was found that only 12 out of the 34 fit this condition. In another study, the use of beta-Sn and Bi as potential anode materials for the MIBs was investigated by Jin *et al.* [156] using the DFT simulations. For an isolated Mg ion, it was found that diffusion barriers in Sn and Bi are 0.43 and 0.67 eV, respectively. As Mg-Mg ions interact in Sn, the diffusion barrier rises for an isolated Mg ion from 0.43 eV to 0.77 eV. However, the diffusion barrier in the Bi did not appear to have changed. From the dynamic simulations and the calculated energy barriers studies, they found that Bi is a better anode choice with faster charge/discharge rates for the MIB than beta-Sn. The computed DFT studies by Sivaraman *et al.* [157] showed that the MIBs with the graphyne-like boron nitride (G-BNyen) cathode had a larger internal energy change and higher cell voltage values when compared to carbon nanomaterials. The calculated maximum theoretical capacity of G-BNyen was ~939.16 mAh g^{-1}. The findings were assessed in terms of charge transport, structural, energetic, and electrical features and offered suggestions for building better anode materials with higher MIB capacity. Qu *et al.* [158] applied computational design using first principles and benchmarked classical MD simulations to execute chemical modifications and mutations on the bis(trifluoro-methane)sulfonamide(TFSI) anion. Based on their findings, only two novel anions out of 15 novel electrolyte salt anions formed from TFSI with the substitution of sulfur atoms in TFSI and the modification of functional groups were prospective candidates for MIBs. These theoretically created electrolyte salts for MIBs offer information and direction for the synthesis and testing of innovative liquid electrochemical systems.

Zinc-ion battery

Due to their affordability, high level of safety, and high theoretical capacity, rechargeable ZIBs have a lot of potential for energy storage applications [159]. However, during the charge/discharge

process, divalent zinc ions experience strong electrostatic interactions with their host materials, which causes slow reaction kinetics. Therefore, it is crucial to enhance ZIB reaction kinetics to improve electrochemical performance. In their review, Tan *et al.* [160] explained the relationships between electrode/electrolyte characteristics, kinetics and intrinsic mechanism of the reactions, theoretically computed Zn-ion migration pathways, energy barriers and related electrochemistry of ZIBs. It also offered a perspective on the difficulties and opportunities in enhancing the reaction process kinetics, which can provide an in-depth understanding of the charge-storage mechanism of ZIBs and useful guidelines for the development of batteries with fast kinetics for the future.

According to the current research by Wu *et al.* [161], 2D ultrathin VSe_2, which is superior to that of other layered transition metal dichalcogenides, can be an interesting consideration as a cathode material for ZIBs with the remarkable zinc-ion storage ability and exceptional battery performance. DFT simulations revealed a significant metallic signature and an ideal zinc-ion diffusion channel with a 0.91 eV energy barrier for the hopping mechanism.

Spinel, a porous substance, is becoming a more significant electrode material for different batteries. Despite this, they have several issues when employed as cathodes in batteries, including limited ion diffusion and significant expansion. With an accuracy of 91.2 %, Cai *et al.* [162] initially picked 18 spinel candidates that met the MIB and ZIB requirements out of the 3,880 spinel materials using DFT and AIMD methods. After a successful screening process, finally, six spinel structures ($MgNi_2O_4$, $MgMo_2S_4$, $MgCu_2S_4$, $ZnCa_2S_4$, $ZnCu_2O_4$, and $ZnNi_2O_4$) were identified as new, high-performance Mg/Zn cathode materials.

Metal-air batteries

Recently, metal-air batteries have gained popularity due to their high energy densities, cost-effectiveness, and lesser weight than other metal-ion batteries [163,164]. They offer unparalleled energy density and, if harnessed to their fullest potential, can offer breakthroughs in diverse applications [165]. If commercially realized, they are likely to cause market disruptions in the areas of defense [166,167], aviation [168], road transportation (EV, hybrid), medicine, consumer electronics, *etc.* just to name a few. They are likely to catalyze some virgin application areas, unforeseen as of now. Figure 12 represents the schematic of a metal-air battery. During discharge, metal oxidation happens at the anode and reduction of oxygen from ambient air occurs at the cathode.

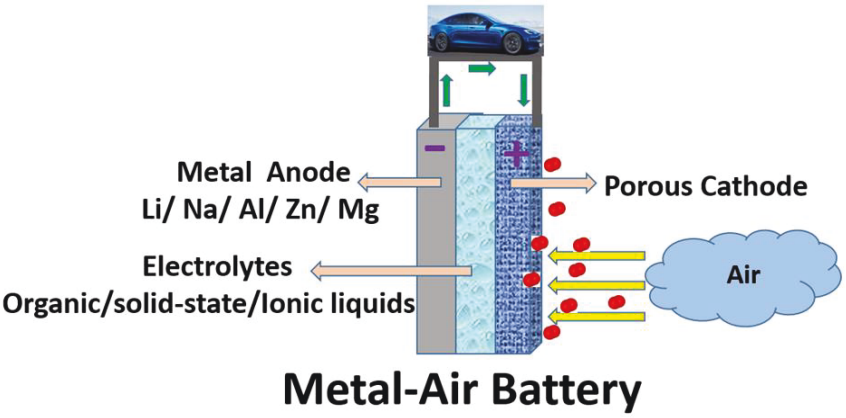

Figure 12. *Schematic of metal-air battery*

The redox reactions are as presented by Equations (7) and (8):

Anodic reaction: $M \leftrightarrow M^{n+} + ne^-$ (7)

Cathodic reaction: $O_2 + 4e^- + 2H_2O \leftrightarrow 4OH^-$ (8)

where M is a metal and n is the oxidation number of that metal. While charging, a reverse reaction occurs where metals are plated on the anode and gaseous oxygen is evolved at the cathode. A comparison of the theoretical energy densities of some of the prominent metal-air battery systems is shown in Figure 13.

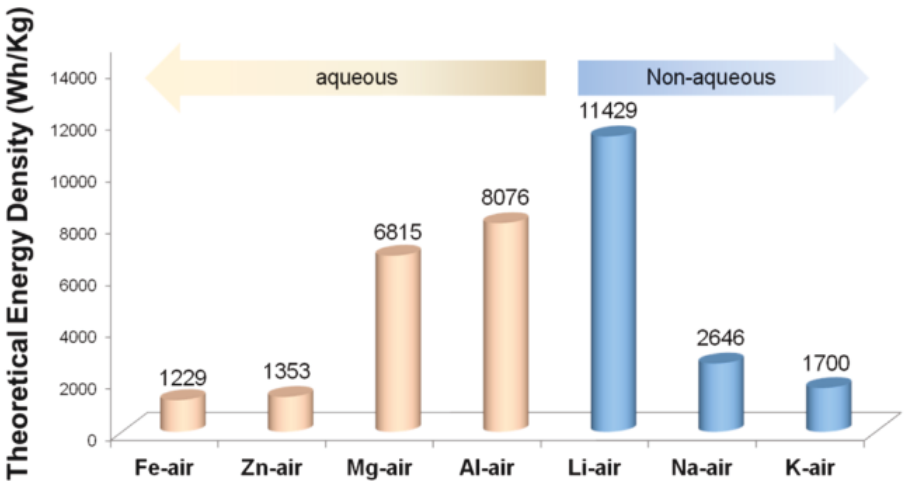

Figure 13. *Theoretical specific energies of various types of metal-air batteries [163]. Copyright 2017. Reproduced with permission from ACS publication*

Li-air battery

The lithium-air battery (LAB) is an excellent option for many application areas because of its highest theoretical specific energy density, as shown in Figure 13. The LAB's most typical design consists of a lithium-metal anode, a lithium-conducting organic electrolyte, and an air electrode supported by carbon. Before they can be used in actual applications, satisfactory resolution for some challenges needs to be found, such as poor catalysis, low conductivity, and degradation of the solvent. Although LABs have been the subject of numerous advanced experimental investigations, it is still not economical enough and have complex electrochemical processes that are difficult to characterize. Computational techniques are used extensively to explore LABs [169,170]. Many intrinsic properties of the constituent materials, such as chemical potential, thermal and electrochemical stability, mobility of the ionic species, and electronic properties, can be estimated with reasonable precession.

The oxygen reduction reaction (ORR) at the oxygen electrode (cathode) of an aprotic Li-air battery was discussed by Hummelshøj *et al.* [171]. They uncovered plausible sources for overpotential during both the charging and discharging processes by using DFT to calculate the free energy of the reaction intermediates. Their findings were validated by the experimental observation that the charge overpotential is much larger than the discharge overpotential. They created a model to study further the electrochemistry of Li-O_2 and the dissolution of Li_2O_2. They identified that for both the discharging and charging, the low thermodynamic overpotentials (0.2 V) are comparable with the low kinetic overpotential seen in tests. To study the fundamental surface chemistry of air cathode catalysts that accelerate the ORR. Xu *et al.* [172] performed periodic DFT calculations with thermodynamic modeling for oxygen reduction by Li on two metal surfaces, Au(111) and Pt(111). According to the findings, Pt(111) stabilizes O more than Li oxide species as compared to Au(111), limiting O reduction's reversible potential. Therefore, they suggested that metal surfaces besides Pt(111) that are more oxophilic could not enhance the reversible potential. Carbon materials like carbon nanotubes and graphene are also attractive as air cathode catalysts. Jing *et al.* [173] explored the initial reduction

reaction on the N-doped graphene surface using DFT and compared it with pristine graphene. Understanding the performance of non-aqueous Li-air batteries requires a thorough understanding of the mechanics and effectiveness of ion transport in Li_2O_2. Radin *et al.* [174] predicted the concentrations and mobilities of charge carriers and intrinsic defects in Li_2O_2 as a function of cell voltage using first-principles calculations. Their calculations showed that variations in the charge state of O_2 dimers control the defect chemistry and conductivity of Li_2O_2. Their research determined that small hole polarons and negative lithium vacancies (missing Li^+) are the primary charge carriers. Despite the attractive features of LABs, like both electrodes were made of lightweight, highly active materials, they still have many technical limitations and safety concerns [175], like those of the LIB. An alternative is to use aqueous metal-air batteries with compatible metals.

Aluminum-air battery

Aluminum, the most plentiful metal in the earth's crust (8 % by mass), having very low atomic weight (important for increasing specific energy density; in the tune of 4140 Wh kg^{-1}), is an important candidate for these aqueous metal-air batteries and has great potential for electric vehicles. However, the experimental OCV is much lower than predicted by bulk thermodynamics. Chen *et al.* [176] studied the thermodynamics of aluminum-air battery (AABs) using DFT. They observed the maximum OCV of only −1.87 V as against the commonly reported value of -2.34 V (for the Al anode) at pH 14.6 Vs the standard hydrogen electrode. These deviations can be largely attributed to the surface processes that alter the electrochemistry of the Al anodic dissolution. They used DFT to study the Al dissolution in alkaline media mediated by a stepwise hydroxide-assisted mechanism through single-electron transfer steps followed by bulk $Al(OH)_3$ formation. The discrepancy in estimating the potential using bulk thermodynamics vs. the one obtained in the stepwise mechanism arises from (i) asymmetry in free energies of intermediates in multielectron transfer reactions and (ii) formation of bulk $Al(OH)_3$ from $Al(OH)_3$ imparts chemical stability.

The problem of high levels of self-corrosion needs to be addressed before AABs can be a commercial success, irrespective of electrolyte types (neutral or alkaline). There are two approaches to address this: (i) addition of elements (like Mg, Mn, Zn, Ga, In, Sn, and Pb) that have higher overpotential (vs. pure aluminum) for the evolution of hydrogen; (ii) using organic/inorganic corrosion inhibitors. The latter might be the preferred choice owing to its cost-effectiveness and facile operational implementation and it is no wonder that many researchers have studied it extensively. The inhibition effect imparted by calcium oxide and L-aspartic hybrid inhibitor for Al alloy anode in alkaline AAB was investigated by Kang *et al.* [177] and the mechanism of inhibition was investigated by DFT combined with MC simulation. Gelman *et al.* introduced the non-aqueous, ionic liquid electrolyte-based Al-air battery. Al ions migrating there during battery discharge caused oxygen reduction, which led to the detection of Al_2O_3 on the air electrode [178]. Crystal orientation was taken into consideration when evaluating the electrochemical aspects of the anode (aluminum, in this case) in an AAB, both theoretically and practically. DFT calculations were made for the (111) and (100) planes of aluminum's open circuit potential in high pH (alkaline) solution. It was observed that the orientation influence and the I-P curve, the Al (100) plane, displayed the highest output power [179].

Zinc-air battery

Among the metal-air battery classes, zinc-air battery (ZAB) is the only commercial success story. Primary zinc-air button cells have been used in hearing aids. Therefore, research on rechargeable ZABs is placed on a very mature scientific foundation. The two primary advantages are: (i) discharge products do not produce a passive layer, and (ii) they have reversible crystallization kinetics. Owing

to these factors, Metallic zinc anodes can withstand repeated cycling spanning a few hundred cycles for over a few months in ambient conditions. The theoretical specific energy density of ZABs reaches 1100 Wh kg^{-1} with respect to the mass of Zn [180].

Apart from the high energy density, ZABs have a few more important traits, *e.g.,* relatively stable discharge potential, much longer storage life, non-reactivity with water, lower costs (owing to relative abundance), and environment-friendly. However, unsolved issues for rechargeable ZABs remain, particularly concerning cycle life and durability. Major technical challenges also include zinc oxide (ZnO) precipitation-induced passivation, morphological changes (shape) of metallic Zn at repeated cycling, and slow reduction of oxygen [181,182].

Stamm *et al.* [183] developed a one-dimensional electrolyte transport model based on thermodynamics for both porous electrodes. The model considers diffusion, migration, and convection. They found that the primary ZABs have issues like inhomogeneous deposition and dissolution of ZnO and Zn, which can be addressed, to some extent, by adding ZnO to Zn even though it has some demerit of reducing initial capacity.

Understanding and alleviating Hydrogen Evolution Reaction (HER) at the negative electrode in a secondary ZAB is a serious issue. Lysgaard *et al.* [184] combined Differential Electrochemical Mass Spectrometry (DEMS) and DFT to understand the contrasting role played by the additives (favorable ones like In and Bi vs. unfavorable Ag) to contain this. The favorable ones spread on the surface, supporting the beneficial effects on Zn dissolution, thereby limiting the HER. Overall, the addition of suitable additives positively impacts the cells' performance when contrasted to cells without it.

Magnesium-air battery

Recently, the rechargeable non-aqueous magnesium-air battery (MAB) is turning out to be an interesting candidate for the next generation secondary battery due to the high theoretical volumetric density (3832 Ah L^{-1} for Mg anode versus 2062 Ah L^{-1} for Li), lower cost and relatively safe operations [185,186]. Bhauriyal *et al.* [187] employed DFT to find the suitability of graphite as a carbon cathode for MABs. Towards that end, they checked the suitability of graphene/graphite for cathode by studying the initial MgO and MgO_2 nucleation processes. Free energy diagrams offer vital clues about the redox reactions of oxygen, which are important to find the rate-determining step that, in turn, controls the initial nucleation of MgO and MgO_2. It was observed that graphene and graphite are roughly similar as far as nucleation of MgO or MgO_2 is concerned, while the overpotential responsible for the controlling of MgO nucleation is relatively higher than that of MgO_2. It is relatively difficult to nucleate MgO and MgO_2 clusters on graphene/graphite surfaces owing to higher overpotential than the MgO or MgO_2 nucleation on pure MgO or MgO_2. They used MD simulations to analyze the MgO_2 nucleation on graphene, which confirmed the selectivity of MgO_2 formation over MgO.

Very low solid-state diffusion of Mg^{2+} is one of the most limiting factors in the commercial realization of rechargeable magnesium (Mg) batteries. Liu *et al.* [188] used MD simulations to investigate the structure and ion transport in a doped-Mg electrode/$MgCl_2$ electrolyte system with a focus on the level of doping. They found that amongst the different candidate electrodes (*i.e.,* Mg-Zn, Mg-Al, Mg-Si, and pure Mg), the Mg-Si strongly attracts the ions in the electrolyte, offering superior performance. They also calculated the capacitances of the negative electrode and electric double-layer (EDL) thickness of different structures. The results showed that the capacitances and EDL thickness have a non-monotonic relationship with the depth of the potential well.

Outlook

Multiple avenues for increasing the safety and performance of LIBs are extensively explored and many of them are likely to be adopted by many industries in the near future. As a competitive substitute for LIB batteries beyond Li, in general, multivalent types, in particular, are considered potential candidates for energy storage systems that can be deployed at large scales. In that regard, strategic computational materials and cell development are anticipated to play significant roles in the analysis and investigation of battery properties in all length scales (atom to device), as shown in Figure 14 and Table 3.

Table 3. *List of different battery properties studied from a computational approach*

Electrode potential	Electron affinity	Porosity	Thermal expansion
Electronic configuration	Electronic structure	Electrode grain boundary	Cell voltage
Electronegativity	Defects engineering	Morphology	State of charge
Spin state	Ionic conductivity	stability	State of health
Ionization potential	Ion-diffusion	Surface structure	Impedance

The research should not be conducted in the isolated silos in academic and industrial R&D arenas alone as has been traditionally done, but in active collaboration with industrial R&D sectors, with a focus on accelerating progress through the creation of useful synergies.

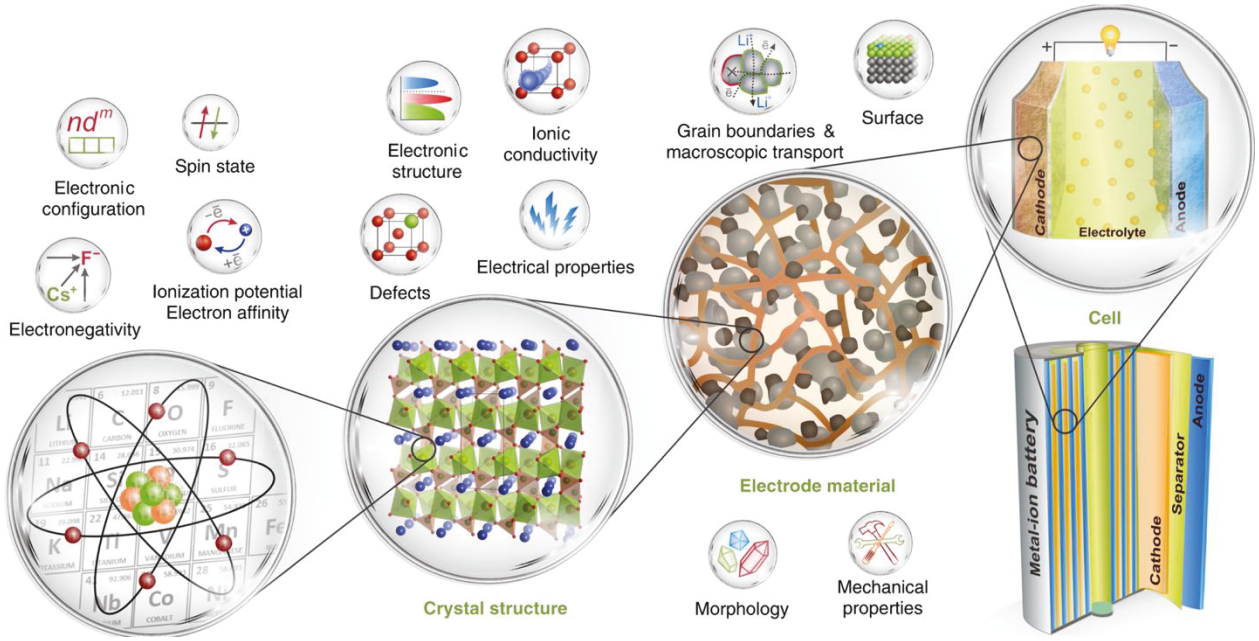

Figure 14. *Summary of computational approach capability for the development for Li- and non-Li advanced battery properties determinations [189]. Copyright 2020. Reproduced with permission from Springer Nature.*

Among various Li/Li-ion-based batteries, Li-S, Li-Si, and Li-Air batteries are the most advantageous and promising. However, some critical challenges must be resolved to bring them to commercial production. The notable challenges include the shuttling effect in Li-S batteries, enhancement of stability and conductivity properties of Si anode, and obtaining cost-effective, stable, and robust catalyst material for Li-Air batteries. These challenges can most effectively be investigated and solved with the help of robust computation tools, which will accelerate the development in terms of time, cost, and safety.

For example, by integrating computational methods like DFT and KMC, it is possible to simulate the dendritic growth and morphology for both LiBs and non-LiBs functioning under diverse external and internal constraints. These investigations are beneficial for both enhancing the performance of rechargeable batteries and preventing short circuits. The performance of advanced LIBs and non-LIBs is strongly governed by their structural and physical properties during spontaneous electrochemical reactions and thus, computational studies are necessary for a comprehensive understanding of the chemistry at the atomic/molecular level. The maturity of computational techniques makes in-depth study possible for available materials for their potential use in batteries with improved accuracy. Additionally, numerous possible composite materials for batteries predicted by AI and ML techniques can be computationally evaluated and experimentally validated to estimate and optimize their performance so that further efforts for commercialization could be concentrated to focus on efficient materials only.

Conflict of interest: *All the authors declare no conflict of interest.*

Acknowledgment: *KKS acknowledges the financial support from UAY (grant no IITBBS_006, phase-I and IITBBS_004, phase-II). HS acknowledges the financial support from NetTantra Technologies India Pvt. Ltd.*

References

[1] W. Chen, J. Liang, Z. Yang, G. Li, A Review of Lithium-Ion Battery for Electric Vehicle Applications and Beyond, *Energy Procedia*. **158** (2019) 4363-4368. https://doi.org/10.1016/j.egypro.2019.01.783

[2] V. Palomares, P. Serras, I. Villaluenga, K. B. Hueso, J. Carretero-González, T. Rojo, Na-ion batteries, recent advances and present challenges to become low cost energy storage systems, *Energy Environ. Sci.* **5** (2012) 5884. https://doi.org/10.1039/c2ee02781j

[3] K. Xu, Nonaqueous Liquid Electrolytes for Lithium-Based Rechargeable Batteries, *Chem. Rev.* **104** (2004) 4303-4418. https://doi.org/10.1021/cr030203g

[4] I. Bloom, B. G. Potter, C. S. Johnson, K. L. Gering, J. P. Christophersen, Effect of cathode composition on impedance rise in high-power lithium-ion cells: Long-term aging results, *J. Power Sources* **155** (2006) 415-419. https://doi.org/10.1016/j.jpowsour.2005.05.008

[5] W. M. Seong, K.-Y. Park, M.H. Lee, S. Moon, K. Oh, H. Park, S. Lee, K. Kang, Abnormal self-discharge in lithium-ion batteries, *Energy Environ. Sci.* **11** (2018) 970-978. https://doi.org/10.1039/C8EE00186C

[6] Y. Chen, Y. Kang, Y. Zhao, L. Wang, J. Liu, Y. Li, Z. Liang, X. He, X. Li, N. Tavajohi, B. Li, A review of lithium-ion battery safety concerns: The issues, strategies, and testing standards, *J. Energy Chem.* **59** (2021) 83-99. https://doi.org/10.1016/j.jechem.2020.10.017

[7] M.D. Slater, D. Kim, E. Lee, C.S. Johnson, Sodium-Ion Batteries, *Adv. Funct. Mater.* **23** (2013) 947-958. https://doi.org/10.1002/adfm.201200691

[8] A. Ponrouch, J. Bitenc, R. Dominko, N. Lindahl, P. Johansson, M.R. Palacin, Multivalent rechargeable batteries, *Energy Storage Mater.* **20** (2019) 253-262. https://doi.org/10.1016/j.ensm.2019.04.012

[9] J. Pan, Y. Y. Xu, H. Yang, Z. Dong, H. Liu, B. Y. Xia, Advanced Architectures and Relatives of Air Electrodes in Zn-Air Batteries, *Adv. Sci.* **5** (2018) 1700691. https://doi.org/10.1002/advs.201700691

[10] J. Verma, D. Kumar, Metal-ion batteries for electric vehicles: current state of the technology, issues and future perspectives, *Nanoscale Adv.* **3** (2021) 3384-3394. https://doi.org/10.1039/D1NA00214G

[11] P. Hohenberg, W. Kohn, Inhomogeneous Electron Gas, *Phys. Rev.* **136** (1964) B864-B871. https://doi.org/10.1103/PhysRev.136.B864
[12] W. Kohn, L. J. Sham, Self-Consistent Equations Including Exchange and Correlation Effects, *Phys. Rev.* **140** (1965) A1133-A1138. https://doi.org/10.1103/PhysRev.140.A1133
[13] R. Jose, S. Ramakrishna, Materials 4.0: Materials big data enabled materials discovery, *Appl. Mater. Today*. **10** (2018) 127-132. https://doi.org/10.1016/j.apmt.2017.12.015
[14] A. Agrawal, A. Choudhary, Deep materials informatics: Applications of deep learning in materials science, *MRS Commun.* **9** (2019) 779-792. https://doi.org/10.1557/mrc.2019.73
[15] J.-M. Tarascon, M. Armand, Issues and challenges facing rechargeable lithium batteries, *Nature*. **414** (2001) 359-367. https://doi.org/10.1038/35104644
[16] A. N. Jansen, A. J. Kahaian, K. D. Kepler, P. A. Nelson, K. Amine, D. W. Dees, D. R. Vissers, M. M. Thackeray, Development of a high-power lithium-ion battery, *J. Power Sources*. **81-82** (1999) 902-905. https://doi.org/10.1016/S0378-7753(99)00268-2
[17] H. Sharma, J. Kreisel, P. Ghosez, First-principles study of $PbTiO_3$ under uniaxial strains and stresses, *Phys. Rev. B*. **90** (2014) 214102. https://doi.org/10.1103/PhysRevB.90.214102
[18] K. Chatterjee, A. D. Pathak, A. Lakma, C. S. Sharma, K. K. Sahu, A. K. Singh, Synthesis, characterization and application of a non-flammable dicationic ionic liquid in lithium-ion battery as electrolyte additive, *Sci. Rep.* **10** (2020) 9606. https://doi.org/10.1038/s41598-020-66341-x
[19] K. Chatterjee, A. D. Pathak, K. K. Sahu, A. K. Singh, New Thiourea-Based Ionic Liquid as an Electrolyte Additive to Improve Cell Safety and Enhance Electrochemical Performance in Lithium-Ion Batteries, *ACS Omega*. **5** (2020) 16681-16689. https://doi.org/10.1021/acsomega.0c01565
[20] T. Zhang, D. Li, Z. Tao, J. Chen, Understanding electrode materials of rechargeable lithium batteries via DFT calculations, *Prog. Nat. Sci. Mater. Int.* **23** (2013) 256-272. https://doi.org/10.1016/j.pnsc.2013.04.005
[21] G. Kresse, J. Hafner, molecular dynamics for liquid metals, *Phys. Rev. B*. **47** (1993) 558-561. https://doi.org/10.1103/PhysRevB.47.558
[22] A. García, N. Papior, A. Akhtar, E. Artacho, V. Blum, E. Bosoni, P. Brandimarte, M. Brandbyge, J. I. Cerdá, F. Corsetti, R. Cuadrado, V. Dikan, J. Ferrer, J. Gale, P. García-Fernández, V. M. García-Suárez, S. García, G. Huhs, S. Illera, R. Korytár, P. Koval, I. Lebedeva, L. Lin, P. López-Tarifa, S.G. Mayo, S. Mohr, P. Ordejón, A. Postnikov, Y. Pouillon, M. Pruneda, R. Robles, D. Sánchez-Portal, J. M. Soler, R. Ullah, V. W. Yu, J. Junquera, Siesta: Recent developments and applications, *J. Chem. Phys.* **152** (2020) 204108. https://doi.org/10.1063/5.0005077
[23] B. Delley, An all-electron numerical method for solving the local density functional for polyatomic molecules, *J. Chem. Phys.* **92** (1990) 508-517. https://doi.org/10.1063/1.458452
[24] P. Giannozzi, O. Andreussi, T. Brumme, O. Bunau, M. Buongiorno Nardelli, M. Calandra, R. Car, C. Cavazzoni, D. Ceresoli, M. Cococcioni, N. Colonna, I. Carnimeo, A. Dal Corso, S. de Gironcoli, P. Delugas, R. A. DiStasio, A. Ferretti, A. Floris, G. Fratesi, G. Fugallo, R. Gebauer, U. Gerstmann, F. Giustino, T. Gorni, J. Jia, M. Kawamura, H.-Y. Ko, A. Kokalj, E. Küçükbenli, M. Lazzeri, M. Marsili, N. Marzari, F. Mauri, N. L. Nguyen, H.-V. Nguyen, A. Otero-de-la-Roza, L. Paulatto, S. Poncé, D. Rocca, R. Sabatini, B. Santra, M. Schlipf, A.P. Seitsonen, A. Smogunov, I. Timrov, T. Thonhauser, P. Umari, N. Vast, X. Wu, S. Baroni, Advanced capabilities for materials modelling with Quantum ESPRESSO, *J. Phys. Condens. Matter*. **29** (2017) 465901. https://doi.org/10.1088/1361-648X/aa8f79
[25] X. Gonze, J.-M. Beuken, R. Caracas, F. Detraux, M. Fuchs, G.-M. Rignanese, L. Sindic, M. Verstraete, G. Zerah, F. Jollet, M. Torrent, A. Roy, M. Mikami, Ph. Ghosez, J.-Y. Raty, D.C.

Allan, First-principles computation of material properties: the ABINIT software project, *Comput. Mater. Sci.* **25** (2002) 478-492. https://doi.org/10.1016/S0927-0256(02)00325-7

[26] F. Legrain, O. I. Malyi, S. Manzhos, Comparative computational study of the energetics of Li, Na, and Mg storage in amorphous and crystalline silicon, *Comput. Mater. Sci.* **94** (2014) 214-217. https://doi.org/10.1016/j.commatsci.2014.04.010

[27] C.-Y. Chou, M. Lee, G. S. Hwang, A Comparative First-Principles Study on Sodiation of Silicon, Germanium, and Tin for Sodium-Ion Batteries, *J. Phys. Chem. C* **119** (2015) 14843-14850. https://doi.org/10.1021/acs.jpcc.5b01099

[28] Y. Zhao, J. Zhao, Q. Cai, SiC_2 siligraphene as a promising anchoring material for lithium-sulfur batteries: a computational study, *Appl. Surf. Sci.* **440** (2018) 889-896. https://doi.org/10.1016/j.apsusc.2018.01.178

[29] M. Fang, X. Liu, J.-C. Ren, S. Yang, G. Su, Q. Fang, J. Lai, S. Li, W. Liu, Revisiting the anchoring behavior in lithium-sulfur batteries: many-body effect on the suppression of shuttle effect, *npj Comput. Mater.* **6** (2020) 8. https://doi.org/10.1038/s41524-020-0273-1

[30] T. Liu, Z. Jin, D.-X. Liu, C. Du, L. Wang, H. Lin, Y. Li, A density functional theory study of high-performance pre-lithiated MS_2 (M = Mo, W, V) Monolayers as the Anode Material of Lithium Ion Batteries, *Sci. Rep.* **10** (2020) 6897. https://doi.org/10.1038/s41598-020-63743-9

[31] S. Gharehzadeh Shirazi, M. Nasrollahpour, M. Vafaee, Investigation of Boron-Doped Graphdiyne as a Promising Anode Material for Sodium-Ion Batteries: A Computational Study, *ACS Omega*. **5** (2020) 10034-10041. https://doi.org/10.1021/acsomega.0c00422

[32] A. H. Farokh Niaei, T. Hussain, M. Hankel, D. J. Searles, Hydrogenated defective graphene as an anode material for sodium and calcium ion batteries: A density functional theory study, *Carbon*. **136** (2018) 73-84. https://doi.org/10.1016/j.carbon.2018.04.034

[33] M. Riyaz, S. Garg, N. Kaur, N. Goel, Boron doped graphene as anode material for Mg ion battery: A DFT study, *Comput. Theor. Chem.* **1214** (2022) 113757. https://doi.org/10.1016/j.comptc.2022.113757

[34] M. I. Khan, G. Nadeem, A. Majid, M. Shakil, A DFT study of bismuthene as anode material for alkali-metal (Li/Na/K)-ion batteries, *Mater. Sci. Eng. B* **266** (2021) 115061. https://doi.org/10.1016/j.mseb.2021.115061

[35] S. Bertolini, T. Jacob, Density Functional Theory Studies on Sulfur-Polyacrylonitrile as a Cathode Host Material for Lithium-Sulfur Batteries, *ACS Omega* **6** (2021) 9700-9708. https://doi.org/10.1021/acsomega.0c06240

[36] O. I. Malyi, K. Sopiha, V. V. Kulish, T. L. Tan, S. Manzhos, C. Persson, A computational study of Na behavior on graphene, *Appl. Surf. Sci.* **333** (2015) 235-243. https://doi.org/10.1016/j.apsusc.2015.01.236

[37] K. C. Wasalathilake, G. A. Ayoko, C. Yan, Effects of heteroatom doping on the performance of graphene in sodium-ion batteries: A density functional theory investigation, *Carbon*. **140** (2018) 276-285. https://doi.org/10.1016/j.carbon.2018.08.071

[38] V. L. Chevrier, J. W. Zwanziger, J. R. Dahn, First principles studies of silicon as a negative electrode material for lithium-ion batteries, *Can. J. Phys.* **87** (2009) 625-632. https://doi.org/10.1139/P09-031

[39] S. Loftager, J. M. García-Lastra, T. Vegge, A Density Functional Theory Study of the Ionic and Electronic Transport Mechanisms in $LiFeBO_3$ Battery Electrodes, *J. Phys. Chem. C* **120** (2016) 18355-18364. https://doi.org/10.1021/acs.jpcc.6b03456

[40] X. He, Q. Bai, Y. Liu, A. M. Nolan, C. Ling, Y. Mo, Crystal Structural Framework of Lithium Super-Ionic Conductors, *Adv. Energy Mater.* **9** (2019) 1902078. https://doi.org/10.1002/aenm.201902078

[41] I. Levin, NIST Inorganic Crystal Structure Database (ICSD), (2020). https://doi.org/10.18434/M32147 (accessed October 19, 2023)
[42] J. A. Dawson, P. Canepa, T. Famprikis, C. Masquelier, M. S. Islam, Atomic-Scale Influence of Grain Boundaries on Li-Ion Conduction in Solid Electrolytes for All-Solid-State Batteries, *J. Am. Chem. Soc.* **140** (2018) 362-368. https://doi.org/10.1021/jacs.7b10593
[43] E. M. Gavilán-Arriazu, M. P. Mercer, D. E. Barraco, H. E. Hoster, E. P. M. Leiva, Kinetic Monte Carlo simulations applied to Li-ion and post Li-ion batteries: a key link in the multi-scale chain, *Prog. Energy*. **3** (2021) 042001. https://doi.org/10.1088/2516-1083/ac1a65
[44] L. Zhang, S. Chen, W. Wang, H. Yu, H. Xie, H. Wang, S. Yang, C. Zhang, X. Liu, Enabling dendrite-free charging for lithium batteries based on transport-reaction competition mechanism in CHAIN framework, *J. Energy Chem.* **75** (2022) 408-421. https://doi.org/10.1016/j.jechem.2022.09.007
[45] X. Chen, B. Zhao, C. Yan, Q. Zhang, Review on Li Deposition in Working Batteries: From Nucleation to Early Growth, *Adv. Mater.* **33** (2021) 2004128. https://doi.org/10.1002/adma.202004128
[46] Y. Lu, C. Zhao, H. Yuan, X. Cheng, J. Huang, Q. Zhang, Critical Current Density in Solid-State Lithium Metal Batteries: Mechanism, Influences, and Strategies, *Adv. Funct. Mater.* **31** (2021) 2009925. https://doi.org/10.1002/adfm.202009925
[47] J. Liu, H. Yuan, H. Liu, C. Zhao, Y. Lu, X. Cheng, J. Huang, Q. Zhang, Unlocking the Failure Mechanism of Solid State Lithium Metal Batteries, *Adv. Energy Mater.* **12** (2022) 2100748. https://doi.org/10.1002/aenm.202100748
[48] B. Ghalami Choobar, H. Modarress, R. Halladj, S. Amjad-Iranagh, Electrodeposition of lithium metal on lithium anode surface, a simulation study by: Kinetic Monte Carlo-embedded atom method, *Comput. Mater. Sci.* **192** (2021) 110343. https://doi.org/10.1016/j.commatsci.2021.110343
[49] A. Kopač Lautar, D. Kopač, T. Rejec, T. Bančič, R. Dominko, Morphology evolution of magnesium facets: DFT and KMC simulations, *Phys. Chem. Chem. Phys.* **21** (2019) 2434-2442. https://doi.org/10.1039/C8CP06171H
[50] S. K. Kolli, A. Van der Ven, Elucidating the Factors That Cause Cation Diffusion Shutdown in Spinel-Based Electrodes, *Chem. Mater.* **33** (2021) 6421-6432. https://doi.org/10.1021/acs.chemmater.1c01668
[51] R. N. Methekar, P. W. C. Northrop, K. Chen, R. D. Braatz, V. R. Subramanian, Kinetic Monte Carlo Simulation of Surface Heterogeneity in Graphite Anodes for Lithium-Ion Batteries: Passive Layer Formation, *J. Electrochem. Soc.* **158** (2011) A363. https://doi.org/10.1149/1.3548526
[52] N. Sitapure, H. Lee, F. Ospina-Acevedo, P. B. Balbuena, S. Hwang, J. S. Kwon, A computational approach to characterize formation of a passivation layer in lithium metal anodes, *AIChE J.* **67** (2021). https://doi.org/10.1002/aic.17073
[53] Z. Deng, T. P. Mishra, E. Mahayoni, Q. Ma, A. J. K. Tieu, O. Guillon, J.-N. Chotard, V. Seznec, A. K. Cheetham, C. Masquelier, G. S. Gautam, P. Canepa, Fundamental investigations on the sodium-ion transport properties of mixed polyanion solid-state battery electrolytes, *Nat. Commun.* **13** (2022) 4470. https://doi.org/10.1038/s41467-022-32190-7
[54] Y. Onabuta, M. Kunimoto, S. Wang, Y. Fukunaka, H. Nakai, T. Homma, Effect of Li^+ Addition during Initial Stage of Electrodeposition Process on Nucleation and Growth of Zn, *J. Electrochem. Soc.* **169** (2022) 092504. https://doi.org/10.1149/1945-7111/ac8c03
[55] J. Wei, X. Chu, X. Sun, K. Xu, H. Deng, J. Chen, Z. Wei, M. Lei, Machine learning in materials science, *InfoMat*. **1** (2019) 338-358. https://doi.org/10.1002/inf2.12028

[56] G. R. Schleder, A. C. M. Padilha, C. M. Acosta, M. Costa, A. Fazzio, From DFT to machine learning: recent approaches to materials science-a review, *J. Phys. Mater.* **2** (2019) 032001. https://doi.org/10.1088/2515-7639/ab084b

[57] G. Pilania, C. Wang, X. Jiang, S. Rajasekaran, R. Ramprasad, Accelerating materials property predictions using machine learning, *Sci. Rep.* **3** (2013) 2810. https://doi.org/10.1038/srep02810

[58] D. Jha, K. Choudhary, F. Tavazza, W. Liao, A. Choudhary, C. Campbell, A. Agrawal, Enhancing materials property prediction by leveraging computational and experimental data using deep transfer learning, *Nat. Commun.* **10** (2019) 5316. https://doi.org/10.1038/s41467-019-13297-w

[59] R. Ramprasad, R. Batra, G. Pilania, A. Mannodi-Kanakkithodi, C. Kim, Machine learning in materials informatics: recent applications and prospects, *npj Comput. Mater.* **3** (2017) 54. https://doi.org/10.1038/s41524-017-0056-5

[60] A. Dave, J. Mitchell, K. Kandasamy, H. Wang, S. Burke, B. Paria, B. Póczos, J. Whitacre, V. Viswanathan, Autonomous Discovery of Battery Electrolytes with Robotic Experimentation and Machine Learning, *Cell Rep. Phys. Sci.* **1** (2020) 100264. https://doi.org/10.1016/j.xcrp.2020.100264

[61] G. H. Gu, J. Noh, I. Kim, Y. Jung, Machine learning for renewable energy materials, *J. Mater. Chem. A*. **7** (2019) 17096-17117. https://doi.org/10.1039/C9TA02356A

[62] B. Sanchez-Lengeling, A. Aspuru-Guzik, Inverse molecular design using machine learning: Generative models for matter engineering, *Science* **361** (2018) 360-365. https://doi.org/10.1126/science.aat2663

[63] E. Kim, K. Huang, S. Jegelka, E. Olivetti, Virtual screening of inorganic materials synthesis parameters with deep learning, *npj Comput. Mater.* **3** (2017) 53. https://doi.org/10.1038/s41524-017-0055-6

[64] K. T. Butler, D. W. Davies, H. Cartwright, O. Isayev, A. Walsh, Machine learning for molecular and materials science, *Nature* **559** (2018) 547-555. https://doi.org/10.1038/s41586-018-0337-2

[65] Y. Liu, B. Guo, X. Zou, Y. Li, S. Shi, Machine learning assisted materials design and discovery for rechargeable batteries, *Energy Storage Mater.* **31** (2020) 434-450. https://doi.org/10.1016/j.ensm.2020.06.033

[66] C. Chen, Y. Zuo, W. Ye, X. Li, Z. Deng, S. P. Ong, A Critical Review of Machine Learning of Energy Materials, *Adv. Energy Mater.* **10** (2020) 1903242. https://doi.org/10.1002/aenm.201903242

[67] Li-ion Battery Aging Datasets, (2023). https://data.nasa.gov/dataset/Li-ion-Battery-Aging-Datasets/uj5r-zjdb (accessed October 19, 2023)

[68] B. Meredig, A. Agrawal, S. Kirklin, J. E. Saal, J. W. Doak, A. Thompson, K. Zhang, A. Choudhary, C. Wolverton, Combinatorial screening for new materials in unconstrained composition space with machine learning, *Phys. Rev. B*. **89** (2014) 094104. https://doi.org/10.1103/PhysRevB.89.094104

[69] N. Kireeva, V. S. Pervov, Materials space of solid-state electrolytes: unraveling chemical composition-structure-ionic conductivity relationships in garnet-type metal oxides using cheminformatics virtual screening approaches, *Phys. Chem. Chem. Phys.* **19** (2017) 20904-20918. https://doi.org/10.1039/C7CP00518K

[70] S. Manna, D. Roy, S. Das, B. Pathak, Capacity prediction of K-ion batteries: a machine learning based approach for high throughput screening of electrode materials, *Mater. Adv.* **3** (2022) 7833-7845. https://doi.org/10.1039/D2MA00746K

[71] A. Jain, S.P. Ong, G. Hautier, W. Chen, W. D. Richards, S. Dacek, S. Cholia, D. Gunter, D. Skinner, G. Ceder, K.A. Persson, Commentary: The Materials Project: A materials genome

approach to accelerating materials innovation, *APL Mater.* **1** (2013) 011002. https://doi.org/10.1063/1.4812323

[72] Y. Zhang, X. He, Z. Chen, Q. Bai, A. M. Nolan, C. A. Roberts, D. Banerjee, T. Matsunaga, Y. Mo, C. Ling, Unsupervised discovery of solid-state lithium ion conductors, *Nat. Commun.* **10** (2019) 5260. https://doi.org/10.1038/s41467-019-13214-1

[73] X. Chen, L. Ye, Y. Wang, X. Li, Beyond Expert-Level Performance Prediction for Rechargeable Batteries by Unsupervised Machine Learning, *Adv. Intell. Syst.* **1** (2019) 1900102. https://doi.org/10.1002/aisy.201900102

[74] X. Li, J. Li, A. Abdollahi, T. Jones, Data-driven Thermal Anomaly Detection for Batteries using Unsupervised Shape Clustering, *2021 IEEE 30th Int. Symp. Ind. Electron. ISIE*, IEEE, Kyoto, Japan, 2021, pp. 1-6. https://doi.org/10.1109/ISIE45552.2021.9576348

[75] M. V. Reddy, A. Mauger, C. M. Julien, A. Paolella, K. Zaghib, Brief History of Early Lithium-Battery Development, *Materials*. **13** (2020) 1884. https://doi.org/10.3390/ma13081884

[76] J. S. Edge, S. O'Kane, R. Prosser, N. D. Kirkaldy, A. N. Patel, A. Hales, A. Ghosh, W. Ai, J. Chen, J. Yang, S. Li, M.-C. Pang, L. Bravo Diaz, A. Tomaszewska, M. W. Marzook, K. N. Radhakrishnan, H. Wang, Y. Patel, B. Wu, G. J. Offer, Lithium ion battery degradation: what you need to know, *Phys. Chem. Chem. Phys.* **23** (2021) 8200-8221. https://doi.org/10.1039/D1CP00359C

[77] X. Yang, A. L. Rogach, Electrochemical Techniques in Battery Research: A Tutorial for Nonelectrochemists, *Adv. Energy Mater.* **9** (2019) 1900747. https://doi.org/10.1002/aenm.201900747

[78] M.-K. Tran, A. DaCosta, A. Mevawalla, S. Panchal, M. Fowler, Comparative Study of Equivalent Circuit Models Performance in Four Common Lithium-Ion Batteries: LFP, NMC, LMO, NCA, *Batteries* **7** (2021) 51. https://doi.org/10.3390/batteries7030051

[79] Z. Liang, J. Shen, X. Xu, F. Li, J. Liu, B. Yuan, Y. Yu, M. Zhu, Advances in the Development of Single-Atom Catalysts for High-Energy-Density Lithium-Sulfur Batteries, *Adv. Mater.* **34** (2022) 2200102. https://doi.org/10.1002/adma.202200102

[80] J. H. Kim, K. Fu, J. Choi, K. Kil, J. Kim, X. Han, L. Hu, U. Paik, Encapsulation of S/SWNT with PANI Web for Enhanced Rate and Cycle Performance in Lithium Sulfur Batteries, *Sci. Rep.* **5** (2015) 8946. https://doi.org/10.1038/srep08946

[81] L. Zhou, D.L. Danilov, R. Eichel, P. H. L. Notten, Host Materials Anchoring Polysulfides in Li-S Batteries Reviewed, *Adv. Energy Mater.* **11** (2021) 2001304. https://doi.org/10.1002/aenm.202001304

[82] Y. V. Mikhaylik, J. R. Akridge, Polysulfide Shuttle Study in the Li/S Battery System, *J. Electrochem. Soc.* **151** (2004) A1969. https://doi.org/10.1149/1.1806394

[83] D. Moy, A. Manivannan, S. R. Narayanan, Direct Measurement of Polysulfide Shuttle Current: A Window into Understanding the Performance of Lithium-Sulfur Cells, *J. Electrochem. Soc.* **162** (2015) A1-A7. https://doi.org/10.1149/2.0181501jes

[84] K. Kumaresan, Y. Mikhaylik, R. E. White, A Mathematical Model for a Lithium-Sulfur Cell, *J. Electrochem. Soc.* **155** (2008) A576. https://doi.org/10.1149/1.2937304

[85] J. P. Neidhardt, D. N. Fronczek, T. Jahnke, T. Danner, B. Horstmann, W.G. Bessler, A Flexible Framework for Modeling Multiple Solid, Liquid and Gaseous Phases in Batteries and Fuel Cells, *J. Electrochem. Soc.* **159** (2012) A1528-A1542. https://doi.org/10.1149/2.023209jes

[86] M. Marinescu, T. Zhang, G.J. Offer, A zero dimensional model of lithium-sulfur batteries during charge and discharge, *Phys. Chem. Chem. Phys.* **18** (2016) 584-593. https://doi.org/10.1039/C5CP05755H

[87] G. Minton, R. Purkayastha, L. Lue, A Non-Electroneutral Model for Complex Reaction-Diffusion Systems Incorporating Species Interactions, *J. Electrochem. Soc.* **164** (2017) E3276-E3290. https://doi.org/10.1149/2.0281711jes

[88] A. Nazir, H. T. T. Le, C.-W. Min, A. Kasbe, J. Kim, C.-S. Jin, C.-J. Park, Coupling of a conductive Ni_3 (2,3,6,7,10,11-hexaiminotriphenylene) $_2$ metal-organic framework with silicon nanoparticles for use in high-capacity lithium-ion batteries, *Nanoscale* **12** (2020) 1629-1642. https://doi.org/10.1039/C9NR08038D

[89] J. W. Choi, D. Aurbach, Promise and reality of post-lithium-ion batteries with high energy densities, *Nat. Rev. Mater.* **1** (2016) 16013. https://doi.org/10.1038/natrevmats.2016.13

[90] Q. Wang, M. Zhu, G. Chen, N. Dudko, Y. Li, H. Liu, L. Shi, G. Wu, D. Zhang, High-Performance Microsized Si Anodes for Lithium-Ion Batteries: Insights into the Polymer Configuration Conversion Mechanism, *Adv. Mater.* **34** (2022) 2109658. https://doi.org/10.1002/adma.202109658

[91] Z. Yan, S. Yi, X. Li, J. Jiang, D. Yang, N. Du, A scalable silicon/graphite anode with high silicon content for high-energy lithium-ion batteries, *Mater. Today Energy*. **31** (2023) 101225. https://doi.org/10.1016/j.mtener.2022.101225

[92] S. Mei, S. Guo, B. Xiang, J. Deng, J. Fu, X. Zhang, Y. Zheng, B. Gao, P.K. Chu, K. Huo, Enhanced ion conductivity and electrode-electrolyte interphase stability of porous Si anodes enabled by silicon nitride nanocoating for high-performance Li-ion batteries, *J. Energy Chem.* **69** (2022) 616-625. https://doi.org/10.1016/j.jechem.2022.02.002

[93] A. Nazir, H. T. T. Le, A. Kasbe, C.-J. Park, Si nanoparticles confined within a conductive 2D porous Cu-based metal-organic framework (Cu3(HITP)2) as potential anodes for high-capacity Li-ion batteries, *Chem. Eng. J.* **405** (2021) 126963. https://doi.org/10.1016/j.cej.2020.126963

[94] Y. Ren, X. Yin, R. Xiao, T. Mu, H. Huo, P. Zuo, Y. Ma, X. Cheng, Y. Gao, G. Yin, Y. Li, C. Du, Layered porous silicon encapsulated in carbon nanotube cage as ultra-stable anode for lithium-ion batteries, *Chem. Eng. J.* **431** (2022) 133982. https://doi.org/10.1016/j.cej.2021.133982

[95] M. Rashad, H. Geaney, Vapor-solid-solid growth of silicon nanowires using magnesium seeds and their electrochemical performance in Li-ion battery anodes, *Chem. Eng. J.* **452** (2023) 139397. https://doi.org/10.1016/j.cej.2022.139397

[96] Y. Zheng, J. Ma, X. He, Y. Gan, J. Zhang, Y. Xia, W. Zhang, H. Huang, Fe_3O_4 Contribution to Core-Shell Structured Si@C Nanospheres as High-Performance Anodes for Lithium-Ion Batteries, *J. Electron. Mater.* **52** (2023) 1730-1739. https://doi.org/10.1007/s11664-022-10153-4

[97] W. An, P. He, Z. Che, C. Xiao, E. Guo, C. Pang, X. He, J. Ren, G. Yuan, N. Du, D. Yang, D.-L. Peng, Q. Zhang, Scalable Synthesis of Pore-Rich Si/C@c Core-Shell-Structured Microspheres for Practical Long-Life Lithium-Ion Battery Anodes, *ACS Appl. Mater. Interfaces*. **14** (2022) 10308-10318. https://doi.org/10.1021/acsami.1c22656

[98] X. Huang, J. Yang, S. Mao, J. Chang, P. B. Hallac, C. R. Fell, B. Metz, J. Jiang, P. T. Hurley, J. Chen, Controllable Synthesis of Hollow Si Anode for Long-Cycle-Life Lithium-Ion Batteries, *Adv. Mater.* **26** (2014) 4326-4332. https://doi.org/10.1002/adma.201400578

[99] X. Zhou, J. Tang, J. Yang, J. Xie, L. Ma, Silicon@carbon hollow core-shell heterostructures novel anode materials for lithium ion batteries, *Electrochim. Acta* **87** (2013) 663-668. https://doi.org/10.1016/j.electacta.2012.10.008

[100] Y.-S. Choi, J.-H. Park, J.-P. Ahn, J.-C. Lee, Interfacial Reactions in the Li/Si diffusion couples: Origin of Anisotropic Lithiation of Crystalline Si in Li-Si batteries, *Sci. Rep.* **7** (2017) 14028. https://doi.org/10.1038/s41598-017-14374-0

[101] M. K. Y. Chan, C. Wolverton, J. P. Greeley, First Principles Simulations of the Electrochemical Lithiation and Delithiation of Faceted Crystalline Silicon, *J. Am. Chem. Soc.* **134** (2012) 14362-14374. https://doi.org/10.1021/ja301766z

[102] S. C. Jung, J. W. Choi, Y.-K. Han, Anisotropic Volume Expansion of Crystalline Silicon during Electrochemical Lithium Insertion: An Atomic Level Rationale, *Nano Lett.* **12** (2012) 5342-5347. https://doi.org/10.1021/nl3027197

[103] J. Pan, Q. Zhang, J. Li, M. J. Beck, X. Xiao, Y.-T. Cheng, Effects of stress on lithium transport in amorphous silicon electrodes for lithium-ion batteries, *Nano Energy*. **13** (2015) 192-199. https://doi.org/10.1016/j.nanoen.2015.02.020

[104] H. Wang, H. B. Chew, Nanoscale Mechanics of the Solid Electrolyte Interphase on Lithiated-Silicon Electrodes, *ACS Appl. Mater. Interfaces*. **9** (2017) 25662-25667. https://doi.org/10.1021/acsami.7b07626

[105] Y. Jiang, G. Offer, J. Jiang, M. Marinescu, H. Wang, Voltage Hysteresis Model for Silicon Electrodes for Lithium Ion Batteries, Including Multi-Step Phase Transformations, Crystallization and Amorphization, *J. Electrochem. Soc.* **167** (2020) 130533. https://doi.org/10.1149/1945-7111/abbbba

[106] S. S. Damle, S. Pal, P. N. Kumta, S. Maiti, Effect of silicon configurations on the mechanical integrity of silicon-carbon nanotube heterostructured anode for lithium ion battery: A computational study, *J. Power Sources* **304** (2016) 373-383. https://doi.org/10.1016/j.jpowsour.2015.11.027

[107] S. Dhillon, G. Hernández, N. P. Wagner, A. M. Svensson, D. Brandell, Modelling capacity fade in silicon-graphite composite electrodes for lithium-ion batteries, *Electrochimica Acta*. **377** (2021) 138067. https://doi.org/10.1016/j.electacta.2021.138067

[108] S. Suh, H. Choi, K. Eom, H.-J. Kim, Enhancing the electrochemical properties of a Si anode by introducing cobalt metal as a conductive buffer for lithium-ion batteries, *J. Alloys Compd.* **827** (2020) 154102. https://doi.org/10.1016/j.jallcom.2020.154102

[109] C. Min, A. Nazir, H. T. T. Le, C. Park, Facile Fabrication of Highly Porous 3D Sponge-Like Si@C Composites as High-Performance Anode Materials for Lithium-Ion Batteries, *Batter. Supercaps*. **5** e202100403 (2022). https://doi.org/10.1002/batt.202100403

[110] S.-Y. Kim, A. Ostadhossein, A. C. T. van Duin, X. Xiao, H. Gao, Y. Qi, Self-generated concentration and modulus gradient coating design to protect Si nano-wire electrodes during lithiation, *Phys. Chem. Chem. Phys.* **18** (2016) 3706-3715. https://doi.org/10.1039/C5CP07219K

[111] A. Gao, S. Mukherjee, I. Srivastava, M. Daly, C. V. Singh, Atomistic Origins of Ductility Enhancement in Metal Oxide Coated Silicon Nanowires for Li-Ion Battery Anodes, *Adv. Mater. Interfaces*. **4** (2017) 1700920. https://doi.org/10.1002/admi.201700920

[112] F. Shuang, K. E. Aifantis, A First Molecular Dynamics Study for Modeling the Microstructure and Mechanical Behavior of Si Nanopillars during Lithiation, *ACS Appl. Mater. Interfaces*. **13** (2021) 21310-21319. https://doi.org/10.1021/acsami.1c02977

[113] M. A. Kharadi, G. F. A. Malik, F. A. Khanday, K. A. Shah, S. Mittal, B. K. Kaushik, Review—Silicene: From Material to Device Applications, *ECS J. Solid State Sci. Technol.* **9** (2020) 115031. https://doi.org/10.1149/2162-8777/abd09a

[114] S. Sinha, H. Kim, A.W. Robertson, Preparation and application of 0D-2D nanomaterial hybrid heterostructures for energy applications, *Mater. Today Adv.* **12** (2021) 100169. https://doi.org/10.1016/j.mtadv.2021.100169

[115] J. Zhuang, X. Xu, G. Peleckis, W. Hao, S. X. Dou, Y. Du, Silicene: A Promising Anode for Lithium-Ion Batteries, *Adv. Mater.* **29** (2017) 1606716. https://doi.org/10.1002/adma.201606716

[116] Z. Hu, Q. Liu, S.-L. Chou, S.-X. Dou, Two-Dimensional Material-Based Heterostructures for Rechargeable Batteries, *Cell Rep. Phys. Sci.* **2** (2021) 100286. https://doi.org/10.1016/j.xcrp.2020.100286

[117] A. Y. Galashev, K. A. Ivanichkina, K. P. Katin, M. M. Maslov, Computer Test of a Modified Silicene/Graphite Anode for Lithium-Ion Batteries, *ACS Omega* **5** (2020) 13207-13218. https://doi.org/10.1021/acsomega.0c01240
[118] J. E. Padilha, R. B. Pontes, Free-Standing Bilayer Silicene: The Effect of Stacking Order on the Structural, Electronic, and Transport Properties, *J. Phys. Chem. C* **119** (2015) 3818-3825. https://doi.org/10.1021/jp512489m
[119] M. J. Momeni, M. Mousavi-Khoshdel, E. Targholi, First-principles investigation of adsorption and diffusion of Li on doped silicenes: Prospective materials for lithium-ion batteries, *Mater. Chem. Phys.* **192** (2017) 125-130. https://doi.org/10.1016/j.matchemphys.2017.01.082
[120] A. Y. Galashev, K. A. Ivanichkina, Computational investigation of a promising Si-Cu anode material, *Phys. Chem. Chem. Phys.* **21** (2019) 12310-12320. https://doi.org/10.1039/C9CP01571J
[121] B. Ipaves, J. F. Justo, L. V. C. Assali, Aluminum functionalized few-layer silicene as anode material for alkali metal ion batteries, *Mol. Syst. Des. Eng.* (2023) 10.1039.D2ME00172A. https://doi.org/10.1039/D2ME00172A
[122] A. Y. Galashev, O. R. Rakhmanova, Two-Layer Silicene on the SiC Substrate: Lithiation Investigation in the Molecular Dynamics Experiment, *ChemPhysChem* **23** (2022). https://doi.org/10.1002/cphc.202200250
[123] J. Rehman, X. Fan, A. Samad, W. Zheng, Lithiation and Sodiation of Hydrogenated Silicene: A Density Functional Theory Investigation, *ChemSusChem* **14** (2021) 5460-5469. https://doi.org/10.1002/cssc.202101742
[124] L. Zhao, T. Zhang, W. Li, T. Li, L. Zhang, X. Zhang, Z. Wang, Engineering of sodium-ion batteries: Opportunities and challenges, *Engineering* **24** (2022) 172-183. https://doi.org/10.1016/j.eng.2021.08.032
[125] P. K. Nayak, L. Yang, W. Brehm, P. Adelhelm, From Lithium-Ion to Sodium-Ion Batteries: Advantages, Challenges, and Surprises, *Angew. Chem. Int. Ed.* **57** (2018) 102-120. https://doi.org/10.1002/anie.201703772
[126] M. Wang, Q. Wang, X. Ding, Y. Wang, Y. Xin, P. Singh, F. Wu, H. Gao, The prospect and challenges of sodium-ion batteries for low-temperature conditions, *Interdiscip. Mater.* **1** (2022) 373-395. https://doi.org/10.1002/idm2.12040
[127] J. Gu, Z. Zhao, J. Huang, B. G. Sumpter, Z. Chen, MX Anti-MXenes from Non-van der Waals Bulks for Electrochemical Applications: The Merit of Metallicity and Active Basal Plane, *ACS Nano* **15** (2021) 6233-6242. https://doi.org/10.1021/acsnano.0c08429
[128] S. Banerjee, K. Ghosh, S. K. Reddy, S. S. R. K. C. Yamijala, Cobalt Anti-MXenes as Promising Anode Materials for Sodium-Ion Batteries, *J. Phys. Chem. C* **126** (2022) 10298-10308. https://doi.org/10.1021/acs.jpcc.2c02459
[129] F. Wei, S. Xu, J. Li, S. Yuan, B. Jia, S. Gao, G. Liu, P. Lu, Computational Investigation of Two-Dimensional Vanadium Boride Compounds for Na-Ion Batteries, *ACS Omega* **7** (2022) 14765-14771. https://doi.org/10.1021/acsomega.2c00134
[130] A. Moalla, M. Noei, F. Khazali, A. Maleki, A computational study on the BN-yne sheet application in the Na-ion batteries, *J. Mol. Graph. Model.* **97** (2020) 107567. https://doi.org/10.1016/j.jmgm.2020.107567
[131] C. Ye, M. Liu, A computational study on the potential application of carbon nitride nanosheets in Na-ion batteries, *J. Mol. Model.* **28** (2022) 40. https://doi.org/10.1007/s00894-021-05024-4
[132] N. Li, Y. Li, J. Fan, Prediction of chemically ordered dual transition metal carbides (MXenes) as high-capacity anode materials for Na-ion batteries, *Nanoscale* **13** (2021) 7234-7243. https://doi.org/10.1039/D1NR00681A

[133] P. R. Raghuvanshi, M. K. Jangid, A. Bhattacharya, A. Mukhopadhyay, Revealing Na-segregation at the Si/Graphene Interface and Its Implications toward the Na-storage Behavior of Si-Based Electrodes, *ACS Appl. Mater. Interfaces*. **14** (2022) 9667-9675. https://doi.org/10.1021/acsami.1c18748

[134] M. M. Obeid, D. Ni, P.-H. Du, Q. Sun, Design of Three-Dimensional Metallic Biphenylene Networks for Na-Ion Battery Anodes with a Record High Capacity, *ACS Appl. Mater. Interfaces* **14** (2022) 32043-32055. https://doi.org/10.1021/acsami.2c07436

[135] M. Zhou, Y. Shen, J. Liu, L. Lv, X. Gao, X. Wang, X. Meng, X. Yang, Y. Zheng, Z. Zhou, First-principles study on haeckelite hexagonal monolayer with high specific capacity for sodium-ion battery, *Solid State Ion.* **378** (2022) 115898. https://doi.org/10.1016/j.ssi.2022.115898

[136] S. Daryabari, S. Mansouri, J. Beheshtian, M. Karimkhani, A computational study on the novel defects of graphene quantum dot as a promising anode material for sodium ion battery, *Mater. Chem. Phys.* **265** (2021) 124484. https://doi.org/10.1016/j.matchemphys.2021.124484

[137] S. Chu, S. Guo, H. Zhou, Advanced cobalt-free cathode materials for sodium-ion batteries, *Chem. Soc. Rev.* **50** (2021) 13189-13235. https://doi.org/10.1039/D1CS00442E

[138] P. A. Aparicio, J. A. Dawson, M. S. Islam, N. H. de Leeuw, Computational Study of $NaVOPO_4$ Polymorphs as Cathode Materials for Na-Ion Batteries: Diffusion, Electronic Properties, and Cation-Doping Behavior, *J. Phys. Chem. C* **122** (2018) 25829-25836. https://doi.org/10.1021/acs.jpcc.8b07797

[139] G. Snarskis, J. Pilipavičius, D. Gryaznov, L. Mikoliūnaitė, L. Vilčiauskas, Peculiarities of Phase Formation in Mn-Based Na SuperIonic Conductor (NaSICon) Systems: The Case of $Na_{1+2x}Mn_xTi_{2-x}(PO_4)_3$ ($0.0 \leq x \leq 1.5$), *Chem. Mater.* **33** (2021) 8394-8403. https://doi.org/10.1021/acs.chemmater.1c02775

[140] G. Sakata Gurmesa, T. Teshome, N. Ermias Benti, G. Ayalneh Tiruye, A. Datta, Y. Setarge Mekonnen, C. Amente Geffe, Rational Design of Biaxial Tensile Strain for Boosting Electronic and Ionic Conductivities of Na_2MnSiO_4 for Rechargeable Sodium-Ion Batteries, *ChemistryOpen* **11** (2022). https://doi.org/10.1002/open.202100289

[141] B. Peng, Y. Chen, L. Zhao, S. Zeng, G. Wan, F. Wang, X. Zhang, W. Wang, G. Zhang, Regulating the local chemical environment in layered O_3-$NaNi_{0.5}Mn_{0.5}O_2$ achieves practicable cathode for sodium-ion batteries, *Energy Storage Mater.* **56** (2023) 631-641. https://doi.org/10.1016/j.ensm.2023.02.001

[142] R. Rajagopalan, Y. Tang, X. Ji, C. Jia, H. Wang, Advancements and Challenges in Potassium Ion Batteries: A Comprehensive Review, *Adv. Funct. Mater.* **30** (2020) 1909486. https://doi.org/10.1002/adfm.201909486

[143] T. Hosaka, K. Kubota, A. S. Hameed, S. Komaba, Research Development on K-Ion Batteries, *Chem. Rev.* **120** (2020) 6358-6466. https://doi.org/10.1021/acs.chemrev.9b00463

[144] S. Komaba, T. Hasegawa, M. Dahbi, K. Kubota, Potassium intercalation into graphite to realize high-voltage/high-power potassium-ion batteries and potassium-ion capacitors, *Electrochem. Commun.* **60** (2015) 172-175. https://doi.org/10.1016/j.elecom.2015.09.002

[145] Y. Zhu, Y. Yin, X. Yang, T. Sun, S. Wang, Y. Jiang, J. Yan, X. Zhang, Transformation of Rusty Stainless-Steel Meshes into Stable, Low-Cost, and Binder-Free Cathodes for High-Performance Potassium-Ion Batteries, *Angew. Chem. Int. Ed.* **56** (2017) 7881-7885. https://doi.org/10.1002/anie.201702711

[146] C. Zhao, Y. Lu, H. Liu, L. Chen, First-principles computational investigation of nitrogen-doped carbon nanotubes as anode materials for lithium-ion and potassium-ion batteries, *RSC Adv.* **9** (2019) 17299-17307. https://doi.org/10.1039/C9RA03235E

[147] P. Sehrawat, C. Julien, S.S. Islam, Carbon nanotubes in Li-ion batteries, *Mater. Sci. Eng. B*. **213** (2016) 12-40. https://doi.org/10.1016/j.mseb.2016.06.013
[148] S. Yu, S. Kim, H. Kim, W. Choi, Computational screening of anode materials for potassium-ion batteries, *Int. J. Energy Res.* **43** (2019) 7646-7654. https://doi.org/10.1002/er.4771
[149] G. A. Elia, K. Marquardt, K. Hoeppner, S. Fantini, R. Lin, E. Knipping, W. Peters, J.-F. Drillet, S. Passerini, R. Hahn, An Overview and Future Perspectives of Aluminum Batteries, *Adv. Mater.* **28** (2016) 7564-7579. https://doi.org/10.1002/adma.201601357
[150] D. Pal, S. Chakraborty, S. Chattopadhyay, Recent Progress in Al-, K-, and Zn-Ion Batteries: Experimental and Theoretical Viewpoints, *Energy Technol.* **9** (2021) 2100382. https://doi.org/10.1002/ente.202100382
[151] Z. Zhang, X. Zhang, X. Zhao, S. Yao, A. Chen, Z. Zhou, Computational Screening of Layered Materials for Multivalent Ion Batteries, *ACS Omega* **4** (2019) 7822-7828. https://doi.org/10.1021/acsomega.9b00482
[152] M. H. Alfaruqi, S. Islam, J. Lee, J. Jo, V. Mathew, J. Kim, First principles calculations study of α-MnO_2 as a potential cathode for Al-ion battery application, *J. Mater. Chem. A* **7** (2019) 26966-26974. https://doi.org/10.1039/C9TA09321D
[153] J. Li, Q. Liu, R.A. Flores, J. Lemmon, T. Bligaard, DFT simulation of the X-ray diffraction pattern of aluminum-ion-intercalated graphite used as the cathode material of the aluminum-ion battery, *Phys. Chem. Chem. Phys.* **22** (2020) 5969-5975. https://doi.org/10.1039/C9CP06394C
[154] W. Wang, B. Jiang, W. Xiong, H. Sun, Z. Lin, L. Hu, J. Tu, J. Hou, H. Zhu, S. Jiao, A new cathode material for super-valent battery based on aluminium ion intercalation and deintercalation, *Sci. Rep.* **3** (2013) 3383. https://doi.org/10.1038/srep03383
[155] S. Vincent, J. H. Chang, J. M. Garcia Lastra, Computational Design of Ductile Magnesium Alloy Anodes for Magnesium Batteries, *Batter. Supercaps*. **4** (2021) 522-528. https://doi.org/10.1002/batt.202000240
[156] W. Jin, Z. Li, Z. Wang, Y.Q. Fu, Mg ion dynamics in anode materials of Sn and Bi for Mg-ion batteries, *Mater. Chem. Phys.* **182** (2016) 167-172. https://doi.org/10.1016/j.matchemphys.2016.07.019
[157] R. Sivaraman, I. Patra, M. Jade Catalan Opulencia, R. Sagban, H. Sharma, A. Turki Jalil, A. Ghaffar Ebadi, Evaluating the potential of graphene-like boron nitride as a promising cathode for Mg-ion batteries, *J. Electroanal. Chem.* **917** (2022) 116413. https://doi.org/10.1016/j.jelechem.2022.116413
[158] X. Qu, Y. Zhang, N. N. Rajput, A. Jain, E. Maginn, K. A. Persson, Computational Design of New Magnesium Electrolytes with Improved Properties, *J. Phys. Chem. C* **121** (2017) 16126-16136. https://doi.org/10.1021/acs.jpcc.7b04516
[159] C. Li, X. Xie, S. Liang, J. Zhou, Issues and Future Perspective on Zinc Metal Anode for Rechargeable Aqueous Zinc-ion Batteries, *Energy Environ. Mater.* **3** (2020) 146-159. https://doi.org/10.1002/eem2.12067
[160] Y. Tan, F. An, Y. Liu, S. Li, P. He, N. Zhang, P. Li, X. Qu, Reaction kinetics in rechargeable zinc-ion batteries, *J. Power Sources* **492** (2021) 229655. https://doi.org/10.1016/j.jpowsour.2021.229655
[161] Z. Wu, C. Lu, Y. Wang, L. Zhang, L. Jiang, W. Tian, C. Cai, Q. Gu, Z. Sun, L. Hu, Ultrathin VSe_2 Nanosheets with Fast Ion Diffusion and Robust Structural Stability for Rechargeable Zinc-Ion Battery Cathode, *Small* **16** (2020) 2000698. https://doi.org/10.1002/smll.202000698
[162] J. Cai, Z. Wang, S. Wu, Y. Han, J. Li, A Machine Learning Shortcut for Screening the Spinel Structures of Mg/Zn Ion Battery Cathodes with a High Conductivity and Rapid Ion Kinetics, *Energy Storage Mater.* **42** (2021) 277-285. https://doi.org/10.1016/j.ensm.2021.07.042

[163] Y. Li, J. Lu, Metal-Air Batteries: Will They Be the Future Electrochemical Energy Storage Device of Choice?, *ACS Energy Lett.* **2** (2017) 1370-1377. https://doi.org/10.1021/acsenergylett.7b00119

[164] Md. A. Rahman, X. Wang, C. Wen, High Energy Density Metal-Air Batteries: A Review, *J. Electrochem. Soc.* **160** (2013) A1759-A1771. https://doi.org/10.1149/2.062310jes

[165] K. F. Blurton, A. F. Sammells, Metal/air batteries: Their status and potential — a review, *J. Power Sources* **4** (1979) 263-279. https://doi.org/10.1016/0378-7753(79)80001-4

[166] Y. Choi, M. H. Griep, J.-Y. Kim, T.-Y. Ahn, T.R. Park, H.-R. Yu, J.-H. Cho, Lithium-protective hybrid lithium-air batteries with CFx, MoS_2, and WS_2 composite electrodes, *Carbon Lett.* **31** (2021) 331-338. https://doi.org/10.1007/s42823-020-00178-2

[167] J. Goldstein, I. Brown, B. Koretz, New developments in the Electric Fuel Ltd. zinc/air system, *J. Power Sources* **80** (1999) 171-179. https://doi.org/10.1016/S0378-7753(98)00260-2

[168] M. Voskuijl, J. Van Bogaert, A. G. Rao, Analysis and design of hybrid electric regional turboprop aircraft, *CEAS Aeronaut. J.* **9** (2018) 15-25. https://doi.org/10.1007/s13272-017-0272-1

[169] L.-R. Cheng, Z.-Z. Lin, X.-M. Li, X. Chen, 2D $MoSi_2N_4$ as electrode material of Li-air battery — A DFT study, *J. Nanoparticle Res.* **25** (2023) 55. https://doi.org/10.1007/s11051-023-05699-1

[170] F. Fasulo, A. Massaro, A. B. Muñoz-García, M. Pavone, New Insights on Singlet Oxygen Release from Li-Air Battery Cathode: Periodic DFT Versus CASPT2 Embedded Cluster Calculations, *J. Chem. Theory Comput.* **19** (2023) 5210-5220. https://doi.org/10.1021/acs.jctc.3c00393

[171] J. S. Hummelshøj, J. Blomqvist, S. Datta, T. Vegge, J. Rossmeisl, K. S. Thygesen, A. C. Luntz, K. W. Jacobsen, J. K. Nørskov, Communications: Elementary oxygen electrode reactions in the aprotic Li-air battery, *J. Chem. Phys.* **132** (2010) 071101. https://doi.org/10.1063/1.3298994

[172] Y. Xu, W.A. Shelton, O_2 reduction by lithium on Au(111) and Pt(111), *J. Chem. Phys.* **133** (2010) 024703. https://doi.org/10.1063/1.3447381

[173] Y. Jing, Z. Zhou, Computational Insights into Oxygen Reduction Reaction and Initial Li_2O_2 Nucleation on Pristine and N-Doped Graphene in Li-O_2 Batteries, *ACS Catal.* **5** (2015) 4309-4317. https://doi.org/10.1021/acscatal.5b00332

[174] M. D. Radin, D. J. Siegel, Charge transport in lithium peroxide: relevance for rechargeable metal-air batteries, *Energy Environ. Sci.* **6** (2013) 2370. https://doi.org/10.1039/c3ee41632a

[175] N. Imanishi, O. Yamamoto, Perspectives and challenges of rechargeable lithium-air batteries, *Mater. Today Adv.* **4** (2019) 100031. https://doi.org/10.1016/j.mtadv.2019.100031

[176] L.D. Chen, J.K. Nørskov, A.C. Luntz, Al-Air Batteries: Fundamental Thermodynamic Limitations from First-Principles Theory, *J. Phys. Chem. Lett.* **6** (2015) 175-179. https://doi.org/10.1021/jz502422v

[177] Q. X. Kang, Y. Wang, X. Y. Zhang, Experimental and theoretical investigation on calcium oxide and L-aspartic as an effective hybrid inhibitor for aluminum-air batteries, *J. Alloys Compd.* **774** (2019) 1069-1080. https://doi.org/10.1016/j.jallcom.2018.09.391

[178] D. Gelman, B. Shvartsev, Y. Ein-Eli, Aluminum-air battery based on an ionic liquid electrolyte, *J. Mater. Chem. A* **2** (2014) 20237-20242. https://doi.org/10.1039/C4TA04721D

[179] K. M. Kim, S.-R. Choi, J.-G. Kim, Theoretical and Experimental Study of the Crystal Orientation Effect of the Anode on the Aluminum-Air Battery Performance, *J. Electrochem. Soc.* **169** (2022) 120541. https://doi.org/10.1149/1945-7111/acad32

[180] Y. Li, H. Dai, Recent advances in zinc-air batteries, *Chem Soc Rev*. **43** (2014) 5257-5275. https://doi.org/10.1039/C4CS00015C
[181] S. Hosseini, S. Masoudi Soltani, Y.-Y. Li, Current status and technical challenges of electrolytes in zinc-air batteries: An in-depth review, *Chem. Eng. J.* **408** (2021) 127241. https://doi.org/10.1016/j.cej.2020.127241
[182] Z. Zhao, X. Fan, J. Ding, W. Hu, C. Zhong, J. Lu, Challenges in Zinc Electrodes for Alkaline Zinc-Air Batteries: Obstacles to Commercialization, *ACS Energy Lett.* **4** (2019) 2259-2270. https://doi.org/10.1021/acsenergylett.9b01541
[183] J. Stamm, A. Varzi, A. Latz, B. Horstmann, Modeling nucleation and growth of zinc oxide during discharge of primary zinc-air batteries, *J. Power Sources* **360** (2017) 136-149. https://doi.org/10.1016/j.jpowsour.2017.05.073
[184] S. Lysgaard, M. K. Christensen, H. A. Hansen, J. M. García Lastra, P. Norby, T. Vegge, Combined DFT and Differential Electrochemical Mass Spectrometry Investigation of the Effect of Dopants in Secondary Zinc-Air Batteries, *ChemSusChem* **11** (2018) 1933-1941. https://doi.org/10.1002/cssc.201800225
[185] R. Shah, V. Mittal, E. Matsil, A. Rosenkranz, Magnesium-ion batteries for electric vehicles: Current trends and future perspectives, *Adv. Mech. Eng.* **13(3)** (2021) https://doi.org/10.1177/16878140211003398
[186] Q. Guo, W. Zeng, S.-L. Liu, Y.-Q. Li, J.-Y. Xu, J.-X. Wang, Y. Wang, Recent developments on anode materials for magnesium-ion batteries: a review, *Rare Met.* **40** (2021) 290-308. https://doi.org/10.1007/s12598-020-01493-3
[187] P. Bhauriyal, K. S. Rawat, G. Bhattacharyya, P. Garg, B. Pathak, First-Principles Study of Magnesium Peroxide Nucleation for Mg-Air Battery, *Chem. - Asian J.* **13** (2018) 3198-3203. https://doi.org/10.1002/asia.201801057
[188] Y. Liu, H. H. Yan, X. Y. Cui, Underlying Mechanisms of the Electrolyte Structure and Dynamics on the Doped-Anode of Magnesium Batteries Based on the Molecular Dynamics Simulations, *J. Electrochem. Energy Convers. Storage* **18** (2021) 011015. https://doi.org/10.1115/1.4047224
[189] A. M. Abakumov, S. S. Fedotov, E. V. Antipov, J.-M. Tarascon, Solid state chemistry for developing better metal-ion batteries, *Nat. Commun.* **11** (2020) 4976. https://doi.org/10.1038/s41467-020-18736-7